

Tiny-Scale Molecular Structures in The Magellanic Clouds.

I. FUSE, HST and VLT Observations.

M.K. André¹, F. Le Petit^{2,4}, P. Sonnentrucker³, R. Ferlet¹, E. Roueff², T. Civeit¹, J.-M. Désert¹, S. Lacour¹, A. Vidal-Madjar¹

¹ Institut d'Astrophysique de Paris, CNRS/UPMC, 98, bvd ARAGO, 75014 Paris

e-mail: andre@iap.fr

² LUTH and FRE2462 du CNRS, Observatoire de Paris, Place J. Jansen, 921995 Meudon Cedex, France

³ Johns Hopkins University

⁴ Onsala Space Observatory - Se 439 92 - Sweden

the date of receipt and acceptance should be inserted later

Abstract. The objective of this series of two papers is to investigate small-scale molecular structures in the Magellanic Clouds (hereafter MCs). We report on the FUSE detections of the HD and CO molecules **on the lines of sight towards three Large Magellanic stars**: Sk –67D05, Sk –68D135, and Sk –69D246. HD is also detected for the first time **on the lines of sight towards two Small Magellanic Cloud stars**: AV 95 and Sk 159. While the HD and CO abundances are expected to be lower in the Large Magellanic Cloud where molecular fractions are a third of the Galactic value and where the photodissociation flux is up to thousands times larger, we report an average HD/H₂ ratio of 1.4 ± 0.5 ppm and CO/H₂ ratio ranging from 0.8 to 2.7 ppm similar to the Galactic ones. We tentatively identify a deuterium reservoir (hereafter D-reservoir) towards the Small Magellanic Cloud, along the light path to AV 95. We derive a D/H ratio ranging from 1.10^{-6} to 1.110^{-5} . Combining FUSE and HST/STIS data we also analyzed the H₂, CII, CIII, FeII, SII, CI, CI*, and CI** content, when available. High resolution VLT observations of Na I, Ca II, and Ca I were obtained in support of the lower resolution FUSE and STIS data for three targets in order to unravel the sightline velocity structures. These observations form the only such set of detections in the Magellanic Clouds to date and allow us to investigate in **detail** some of the physical properties of the intervening molecular gas. Our observation of the HD and CO molecules in the Magellanic Clouds is an argument for dense ($n_{\text{H}} > 100 \text{ cm}^{-3}$) components. Furthermore, we demonstrate that these components are probably extremely small molecular clumps (possibly as small as 10^2 pc) or filaments similar to the tiny-scale atomic structures (TSAS) recently observed in the halo of our Galaxy by **Richter et al. (2003)**. Interestingly enough, for these five sightlines, we also detected molecular hydrogen originating in the Galactic disk. From these observations, we conclude that tiny-scale molecular filamentary structures are present in the disk of the Galaxy as well.

Key words. ISM: HD molecules, clouds; Galaxies: Magellanic clouds

1. Introduction

For many years, the study of molecular clouds through the CO emission lines has greatly improved our knowledge of the physical properties within the Magellanic Clouds themselves and helped constrain the theoretical models of molecular clouds formation and chemistry in different Galactic environments (Cohen et al. 1988). Over the past decade, in particular, the Swedish-ESO-Submillimeter-Telescope (SEST) has been used to map the radio-emission of molecular complexes within the LMC at an $8.''0$ angular resolution which is an order of magnitude higher compared to previous surveys. Such resolution cor-

responds to a linear extent of about 10 pc at the LMC distance of 50 kpc. The latter survey led to the clear detection of small CO clumps with sizes possibly smaller than 10 pc (Lequeux et al. 1994; Garay et al. 2002), typical densities of a few thousand molecules per cubic centimeter and virial masses around 10^4 solar masses. However, smaller clumps and AU-scale structures, such as those tentatively identified in absorption in the Milky Way (Frail et al. 1994; Lauroesch, Meyer & Blades 2000; Richter, Sembach & Howk 2003) are still out of reach.

An alternative method relies on detailed spectroscopic analyses of selected sightlines that might actually help to unravel such small-scale structures in the Magellanic InterStellar Medium (MC ISM). The high-resolution spec-

troscopic abundance studies of Welty et al. (1999) based on the observations of SN 1987A by Vidal-Madjar et al. (1987) showed that the MC ISM exhibits properties similar to those of the warm, low-density Galactic disk clouds and can contain complex velocity structures with more than 20 components. Some of the absorbers observed toward SN 1987A also showed signatures of relatively cool gas ($T < 1500$ K). The lack of information concerning the molecular content precluded to further characterize this cool phase, however.

With the FUSE data it is now possible to investigate the molecular content of this cool phase as well via H_2 , CO, and HD. Although the HD molecule is the most abundant molecule in the interstellar medium after H_2 , relatively few observations have been reported to date in the Galaxy and few comparisons with theoretical models of translucent clouds have been done (Le Petit et al. 2002). Similarly to H_2 , the **presence of HD** molecule is best determined through its ground state transitions which only occur in the FUV domain. The detection is however difficult due to a low molecular abundance ($\text{HD}/\text{H}_2 \approx 10^{-6}$). The ground-state transitions of HD were first observed with *Copernicus* in the local ISM towards bright, nearby stars (Spitzer & Cochran 1973; Wright & Morton 1979). Only recently did the FUSE mission (Moos et al. 2000) reopen the FUV window with sufficiently high sensitivity to allow the detection of HD further away in the Galactic disk (Ferlet et al. 2000; Rachford et al. 2002; Lacour et al. 2004 in prep.). As to extragalactic search for HD, only two detections were found in the literature, one in the LMC by Bluhm & de Boer (2001) with the FUSE satellite, the other in a Damped Lyman Alpha system towards PKS1232+0.82 (Varshalovich et al. 2001). The conclusions from the work of Bluhm & de Boer (2001) are consistent with the existence of a cool phase in the LMC with molecular abundances (H_2 , HD, CO) typical of Galactic translucent sightlines (Rachford et al. 2002).

The project of this series of two papers is to provide a more extensive knowledge of the “dense”, small-scale molecular structures within the Magellanic Clouds. We wish to point out that we specifically use the term “dense” to designate gas with proton density, n_{H} , above 100 cm^{-3} in this work. In the present paper, emphasis is put on the analysis of H_2 , HD, CO, ClI, ClII, NaI, CaII, SiI, FeII, CI, CI*, and CI**, when available, towards five bright Magellanic Cloud stars. Sk−67D05, Sk−68D135 and Sk−69D246 are located in the LMC. AV95, and Sk159 are in the SMC. In § 2 we describe the reduction of the FUSE, VLT and STIS datasets. The analysis methods used to derive the species column densities are described in § 3. Individual conclusions for each target are presented in § 4. A preliminary discussion of these results is given in § 5 and § 6 summarizes our study.

2. Observations

2.1. FUSE Observations

With the help of the web-based archive maintained at the Institut d’Astrophysique de Paris¹ we have searched for HD lines among the 55 LMC sightlines and 26 SMC sightlines observed with FUSE (see the spectral atlas by Danforth et al. 2002). Each dataset was reprocessed with the CALFUSE pipeline version 2.0.5. The reduction and calibration procedure includes thermal drift correction, geometric distortion correction, heliocentric velocity correction, dead time correction, wavelength and flux calibrations (Sahnow et al. 2000).

The full observation of a given star is often divided into several sub-exposures which are usually aligned by cross-correlation over the entire wavelength domain. However, due to the time-dependent stretching of the wavelength calibration between exposure, coaddition of the entire spectra at once may lead to systematic shifts in the final coadded spectrum. In other words, even though the reference absorption features are perfectly aligned at one end of the spectrum, the global coaddition could result in random shifts at the other end of it. In order to avoid these effects and optimize the coaddition process with the FUSE data, we divided each subexposure into 10 \AA windows and performed the coaddition within these spectral domains, weighting each domain by its exposure time. No coaddition of data from different channels was performed. We however used each channel, independently, in the profile fitting procedure. As a byproduct we computed a basic two components velocity structure (MW+MC) and overplotted a model of the molecular species on top of each spectrum in order to detect the weak HD lines at the MCs velocities.

Finally, out of the 81 MC sightlines observed only five showed detectable amounts of HD; three detections occurred in the LMC (Fig. 1) and two detections occurred in the SMC (Fig. 2). It is important to note that HD is possibly present in a few others lines of sight but could not be detected because of insufficient S/N ratios or large amount of Galactic molecular hydrogen crowding the HD lines arising from the MCs. In Table 1, we report the main stellar and interstellar parameters for each of the five stars. A summary of the FUSE observations is given in Table 2.

2.2. VLT Observations

Spectra of the three LMC targets were obtained at the Very Large Telescope Kueyen at Paranal, Chile, in 2003 April using the Ultraviolet Echelle Spectrograph (UVES, Dekker et al. 2000) in visitor mode (see Table 3). The red and blue arm of UVES, respectively centered at 3900 \AA and 8600 \AA , were used at the same time in dichroic mode during the same night. A non-standard setup was used with the red arm centered at 7500 \AA . We used the $0''.4$ slit to achieve a resolving power of 110,000 (2.6 pixels).

¹ More at <http://fuse.iap.fr>

With these setups we observed the Na I (5890 Å) doublet, Ca I (4230 Å), and Ca II (3930 Å) doublet. 1-D spectra were extracted with the UVES pipeline (Ballester et al. 2000). A careful examination of the corrected 2D images showed that the background and the potential stray light were well corrected with the standard pipeline procedure. However, we noted a shift of the order of 14 km s^{-1} in the wavelength calibration that was corrected using the telluric Na I emission lines (located at 0 km s^{-1} geocentric velocity). S/N ratios of about 30 per pixel were achieved in about 20 minutes.

In order to remove the telluric lines that contaminate the spectra around the Na I doublet (5890 Å), we took an exposure of the well known early type, unreddened star α Vir. We normalized the continuum of all the spectra to unity. We finally divided the normalized LMC spectra by the normalized α Vir spectrum. The absence of telluric lines in the final spectra shown in Figs. 3, 4 and 5 are indicative of the effectiveness and accuracy of our method.

2.3. STIS Observations

One LMC star (Sk-69D246) and one SMC star (AV 95) were previously observed with the HST/STIS instrument using the 140M grating and MAMA detectors (Woodgate et al. 1998; Kimble et al. 1998). The observations contain a complete wavelength coverage from 1150 Å to 1730 Å at 45,800 resolving power (2.0 pixels). The S/N ratios per pixel are about 15 and 10 for Sk-69D246 and AV 95, respectively. We used these medium-resolution (6.5 km s^{-1}) echelle observations to derive the column densities of C I, C I*, C I**, C II, and S II towards both sightlines. A summary of the STIS observations is given in Table 4.

3. Line-of-sight velocity structure

With the exception of the pathlength towards Sk 159 for which little information is available, the detailed interstellar component velocity structure is inferred from high resolution Na I, Ca II, or C II spectra and is given in the heliocentric reference frame. The use of different type of tracers allowed us to better differentiate between cold molecular or purely diffuse atomic components.

3.1. Diffuse gas tracers: Ca II, Ca I, and Na I

We observed the three LMC targets with the VLT with a resolving power of 110,000 around 589 nm, 423 nm, and 393 nm. These observations gave us access to three important species that are usually used in combination to derive the physical conditions of a sightline in the ISM.

The Na I/Ca II ratio for instance can be used as a tracer of the integrated depletion (Welty et al. 1999). Typical values for this ratio in the warm diffuse medium are of the order of -2.0 dex where the Ca is not depleted. In colder, denser clouds (ignoring the shocks), two processes compete to drastically change the Ca II abundance: a severe depletion of calcium onto the grains (by about 2.0

dex) and the decrease of the ionization radiation field that makes of Ca II the dominant ionization stage (Pottasch 1972; Bertin et al. 1993; Welty et al. 1996). In general, in such cold media the Na I/Ca II is found to be as high as 2.5 dex and more. We use this ratio to discriminate between possible diffuse atomic or denser molecular components in the VLT data, thus better constraining the location of the molecular absorbers seen with FUSE at lower resolution.

Ca I is clearly detected towards one of the LMC target: Sk-69D246. In the cooler neutral gas phase where Ca II is the dominant ion stage, the Ca I/Na I ratio can be a useful indicator of the temperature. For $T < 3000 \text{ K}$, $\log N(\text{Ca I})/N(\text{Na I})$ is of the order of -0.1 . At temperatures lower than 1500 K, $\log N(\text{Ca I})/N(\text{Na I})$ is in between -2.5 and -4.5 (Welty et al. 2001). Moreover, if we assume that the ionization equilibrium is reached in the plasma we can, in principle, use the ratio $N(\text{Ca I})/N(\text{Ca II})$ to get a direct estimate of n_e . In the case of the calcium atoms, the relation is simply given by (Welty et al. 1999): $N(\text{Ca I})/N(\text{Ca II}) = n_e/(\Gamma/\alpha)$ where Γ is the photoionization rate and α is the recombination coefficient.

3.2. Molecular gas tracers: C II

Chlorine possesses a unique chemistry in which C II reacts rapidly with H_2 when the latter is optically thick to form HCl^+ , which in turn leads to C I and H I (Jura 1974; Jura & York 1978). Therefore, chlorine is predominantly ionized in H I regions while it is predominantly neutral when cold, optically thick H_2 components are present (Sonnentrucker et al. 2002, 2003).

So far, only four C II lines have experimentally determined f -values (Schectman et al. 1993). Two of these lines (1347 and 1363 Å) appear in the STIS range and the two others (1088 and 1097 Å) in the FUSE range. We have positive detections of C II at 1088 Å for all three LMC stars. Because the 1097 Å line in the LMC gas is often blended with the Galactic components our C II column density estimate relies on the 1088 Å line alone for Sk-67D05, Sk-68D135 and Sk 159. The 1347 Å line was additionally used to constrain the C II column densities towards the two other stars for which archival STIS data exist.

C II exhibits only two transitions, both in the FUSE range at 1063 Å and 1071 Å. The 1063 Å line is often completely obliterated by molecular hydrogen, and hence unusable. The 1071 Å, on the other hand, shows only mild-to-moderate blending with an adjacent H_2 ($J = 4$) line and can therefore be used depending on the sightline complexity. However, the continuum around the latter line is lowered by a broad wind feature. This results in a reduced S/N ratio in that particular spectral region of the spectrum for both the LMC and SMC stars. We, therefore, only report one secure detection of this line towards Sk-69D246 and an upper limit towards Sk-67D05.

4. Analysis

4.1. Profile fitting (PF)

Because of the velocity overlap between the Galactic and the MC features and the low resolution of the FUSE data, many absorption lines are blended. Extensive use of profile fitting methods is therefore mandatory to account for these blends.

The profile fitting program, called *Owens*, is a fortran procedure developed by the FUSE french PI team and is one of the most suitable for studying FUV data (Lemoine et al. 2002). The great advantage of this routine is the ability to fit different spectral domains and various species, simultaneously. Thus, a good b -value estimate can be gained from the comparison of the Doppler broadenings of heavy and light species while, at the same time, blends are naturally resolved. In practice, however, the atomic and molecular species are rarely distributed in a similar way over the same components and a great caution must be used when grouping species together in a single component.

Profile fitting of the atomic and molecular species were thus performed in two independent steps since the atomic absorbers usually show much more complicated velocity structures and larger b -values (more details are given in subsequent sections). Also, data from the different instruments were used at the same time in order to fit simultaneously different species and constrain the different contributions to the doppler broadening (temperature and turbulent velocity). Table 5 is a summary of selected atomic and molecular transitions used in this work.

The other advantage of the *Owens* routine is that it allows to treat as parameters the instrument background, the Point Spread Function (PSF) and possible shifts between spectral windows due to residual errors in the wavelength calibration.

In particular, special care must be taken as to the choice of the PSF when working with the FUSE data. Despite many attempts to characterize the FUSE PSF (Hébrard et al. 2002, Wood et al. 2002), its true shape seems elusive and varying with time. Current values found in the FUSE literature range from a quite optimistic LWRs FWHM of 15 km s^{-1} to 25 km s^{-1} . In our case, we have to coadd individual exposures of the same channel and finally the composite PSF relies on the quality of the coaddition process as well. However, because the S/N of the final data is relatively low, we found that a simple gaussian PSF with 20 km s^{-1} (resolution of 15,000) FWHM worked well and various tests with FWHM 10 % larger or 10 % smaller showed that the PSF plays a minor role in the final error budget largely dominated by the errors on the b -value. Throughout this paper we thus assume the PSF to be independent of the dataset and the observation date.

The errors were derived with the standard χ^2 method as described in Hébrard et al. (2002) and as shown in Fig. 6. We want to outline that, in most of the fits performed, the converged χ^2 are close to unity indicating both that

the fit are consistent with the data and that the data error vector is well estimated by the FUSE pipeline version 2.0.5. However, when the errors are dominated by systematics, a more conservative method needs to be employed. Such was the case for the LMC H_2 $J = 2, 3$ levels that are dominated by small errors in the b -value. For these, we explored the different b -values consistent with the global fit and report the full range of possible values.

4.2. Apparent Optical Depth (AOD)

Both AOD and profile fitting techniques were used to determine $N(\text{HD})$ and $N(\text{CII})$ in order to better understand potential sources of systematic error. The AOD method (Savage & Sembach 1991) yields apparent column densities, N_a , that are equivalent to the true column density if no unresolved saturated structure is present. If such structure is present, then $N_a < N_{\text{PF}}$, and the apparent column density is a lower limit to the true column density. Our AOD analysis, including estimation of the errors, follows the procedures outlined in Savage & Sembach (1991). Note that it was not possible to apply the AOD technique to CO because of a severe blend with one H_2 $J = 4$ Galactic line. This blend was naturally resolved using the profile fitting technique.

4.3. H_2 column densities

We adopted the wavelengths, oscillator strengths, and damping constants for the molecular hydrogen transitions from Abgrall et al. (1993a) for the Lyman system and Abgrall et al. (1993b) for the Werner system. The inverses of the total radiative lifetimes are reported in Abgrall et al. (2000). The profile fitting was performed both in the MW and the MCs over 10 to 20 different spectral regions simultaneously. Rotational levels up to $J = 6$ were considered.

In the MCs, the $J = 0$ and $J = 1$ levels are the most populated levels and show damping wings. The estimates of the total H_2 column densities in the MCs are therefore well constrained by these two levels. The higher J levels, on the other hand, appear to show various degrees of saturation. Thus, prior knowledge of the sightlines velocity structure is mandatory to the analysis of these levels. This preliminary analysis was performed using higher resolution (3 km s^{-1}) VLT optical data of NaI, CaII that trace the most diffuse components and STIS high resolution data of CII that traces the optically thick H_2 components. Indeed, we find that with the exception of Sk -69D246 and Sk 159, the present sightlines are dominated by a single molecular absorber.

The errors were derived following the procedure described in § 3.1. Note however that while cold unresolved components might well still be present in the FUSE spectra, our conclusions based on $J = 0$ and $J = 1$ lines remain unaffected. The total H_2 column density and the kinetic

temperature of this gas (T_{01}) still remain accurately determined.

All of the molecular absorbers detected in the Galaxy have column densities several orders of magnitude smaller than towards the Magellanic Clouds. That is obviously an observational bias due to the severe blending between the Galactic and the Magellanic features. An upper limit to the Galactic H_2 is of the order of $\log N(H_2) \approx 18.0$ dex. Beyond that limit, Magellanic absorption lines start to suffer **from** the strong MW blending.

4.4. HD column density

All the ground state ro-vibrational bands of the HD molecules lie below 1180 Å. The FUSE range is therefore perfectly suited to study this molecule. The wavelengths for the $J = 0$ and 1 rotational levels were taken from Roueff & Zeippen (1999) while the f -values come from the calculations of Abgrall & Roueff (2003). This new set of improved f -values takes into account the rotational coupling between electronic states.

In the LMC, because of the severe blending of most of the HD lines (shifted by about $+250 \text{ km s}^{-1}$) with strong H_2 features from the Milky Way, we could only select a handful of useful spectral domains containing HD ($J = 0$): around 959 Å, 1011 Å, 1043 Å and 1066 Å. Yet, depending on the S/N ratio of a given spectrum and depending on the particular blending between Galactic species and HD along a given sightline, some of these domains had to be discarded for the analysis. As an example, profile fitting of HD in the spectrum of Sk -69D246 is shown in Fig. 5.

Our method of investigation combines AOD measurements of the strongest detected transition (HD $J = 0$ at 1043 Å) with profile fitting performed simultaneously over several spectral domains. Both results are indeed comparable and demonstrate that the HD lines are on the linear part of the curve of growth. Thus, the HD column is not sensitive to the b -value used in the profile fitting method. Each of these methods allows us to get independent measurements, with their own error estimates, that are then compared and averaged.

The situation is the same with HD lines originating in the SMC with the difference that the typical velocity shift is only $+150 \text{ km s}^{-1}$. Towards the SMC, there are only three available HD lines clear of blending at 1007 Å, 1011 Å, and 1043 Å. Again, the final result is the average of a profile fitting and an AOD measurements.

For the sightline towards Sk -69D246, we compared our result with the work of Bluhm & de Boer (2001) towards the LMC. Our HD column density appears to be only half of their claimed value. While they used only 2 transitions of the HD molecule (the 1043 Å and 1066 Å lines) assuming no blending, we fitted 2 additional transitions at 1011 Å and 959 Å with FUSE. Performing simultaneous fits over several windows, we were able to unravel a blend of the 1066 Å line. Indeed, the equivalent width measured at 1066 Å is twice as big as expected from the

measurement of the equivalent width at 1043 Å. To our knowledge, this extra absorption feature does not correspond to any known species either at the MW or at the LMC velocity. Finally we attributed this blend to a stellar line (see Fig. 7). This blend was, hence, responsible for an overestimation of the HD column density published by Bluhm & de Boer (2001).

4.5. CO

Two strong ^{12}CO bands are usually detected in the FUSE spectra, the E-X band at 1076 Å and the ^{12}CO C-X band centered at 1087 Å. We detected the 1087 Å band in the spectra of the LMC sightlines while we tentatively derived upper limits towards the SMC sightlines. The other bands present in the spectra could not be used either because they are too weak or because of blends with a stronger Galactic feature. The f -values were taken from Morton & Noreau (1994) for the 1087 Å line.

The ^{13}CO absorption lines are also located in the FUSE range and are totally blended with the ^{12}CO absorption lines. However, we did not add the ^{13}CO bands in our profile fitting since the ^{13}C isotopes are supposed to be a minute fraction of the total carbon atoms. It is well known that the $^{12}\text{C}/^{13}\text{C}$ ratio is a sensitive indicator of the degree of stellar nucleosynthesis and is expected to decrease with the Galactic chemical evolution (Woolley & Weaver 1995). Since the $^{12}\text{CO}/^{13}\text{CO}$ ratio is of the order of 70 in the Galaxy (Savage et al. 2002) it is clear that ^{13}CO is negligible at the level of accuracy of our analysis.

Our fits include rotational levels up to $J = 3$. Despite the weakness of the band we conducted an investigation of the individual population distribution. Noteworthy is that the CO rotational levels spread over 100 km s^{-1} in the C-X band. It is, hence, possible to partially deblend their different participation to the profile with the FUSE resolution ($\approx 20 \text{ km s}^{-1}$). Rotational levels greater than $J = 4$ are found to be negligible which is consistent with subthermal excitation temperatures ($\approx 4 \text{ K}$) measured in the diffuse Galactic disk (Rachford et al. 2002).

Note that an additional difficulty towards the LMC stars resides in the partial blending of the 1087 Å line with a Galactic H_2 $J = 4$ line and a ClI line. Fortunately the analysis of the Galactic H_2 and ClI makes it possible to safely deblend the LMC CO absorption lines when present.

4.6. Cl, Cl*, and Cl**

Cl absorption lines are present in all our FUSE spectra. However, given that most of these lines are multiplets and that the S/N ratio is not high enough to deblend the absorption lines, it is not possible to derive the relative population of the excited states. The situation is worsened by the potential blend between Galactic and MC Cl absorption lines.

In the case of Sk –69D246 and AV 95, however, the blending can be resolved due to the existence of complementary STIS data that also contain a wealth of carbon lines at higher resolution (see Table 5). We estimate the column densities for the carbon lines and use them to derive the average density of the probed clouds.

The relative population of neutral carbon atoms in excited fine-structure levels of the ground electronic state can be used to estimate the number densities and temperatures of neutral clouds in the ISM (Jenkins & Shaya 1979; Jenkins & Tripp 2001). Using the f_1 – f_2 diagram ($f_1 = N(\text{C I}^*)/N(\text{C I}_{\text{total}})$; $f_2 = N(\text{C I}^{**})/N(\text{C I}_{\text{total}})$), we thus derive the thermal pressures (P/k) towards AV 95 and Sk-69D246. Assuming that the carbon lines are arising in the dense molecular component with a temperature $T = T_{01}(\text{H}_2)$ we can then infer the average H number density, n_{H} of the medium crossed (see Table 6 and sections below).

5. Results for individual sightlines

5.1. Sk –67D05

Sk –67D05 is a O9.7Ib star (Neubig, Bruhweiler & Smith 1999; Tumlinson et al. 2002) located near the Western edge of the LMC. It lies in a diffuse H II region (Chu et al. 1994) with relatively low diffuse X-ray emission (Snowden & Petre 1994). The sightline towards Sk –67D05 was the first LMC target investigated with FUSE showing large amount of molecular hydrogen (Friedman et al. 2000). Fits of the Na I and Ca II lines reveal up to 12 components in four distinct groups as shown in Fig. 3: the Galactic group centered at 0 km s^{–1}, an Intermediate Velocity Cloud (IVC) at +77 km s^{–1}, and High Velocity Cloud (HVC) at +144 km s^{–1}, and the LMC group centered at +280 km s^{–1}. Our VLT data show the hidden complexity behind the simple picture derived at lower resolution (15,000) by Friedman et al. (2000) using FUSE data alone. A detailed summary of these Na I and Ca II components is given in Table 7.

The lack of Na I absorbers in between the IVC and HVC groups is quite remarkable for an LMC target since large absorptions at $\approx +60$ km s^{–1} and $\approx +120$ km s^{–1} are usually observed along LMC sightlines. However, in their survey of Magellanic sightlines with IUE, Savage & de Boer (1981) reported the detection of an IVC and a HVC clouds in the light path to Sk –67D05 through low ions absorptions (Mg I, O I, Si II, and Fe II). Danforth et al. (2002) recently confirmed the galactic origin of these absorbers from a deep investigation of dozens of FUSE LMC sightlines. They demonstrated that both the IVC and the HVC are located in the general direction of the Eastern edge of the LMC so that the Western line of sight towards Sk –67D05 is likely sampling only a small fraction of this material.

Molecular hydrogen absorption lines are detected in the FUSE data. Rotational levels up to $J = 3$ were detected in the MW group and up to $J = 6$ in the LMC

group. Because some of the molecular hydrogen absorption lines are expected to be saturated, it is mandatory to use as much information as possible on the velocity structure of the molecular components. Although we do not have direct information from molecular tracer species with our high resolution VLT data, the detailed investigation of the Na I and the Ca II lines is used to infer a plausible molecular velocity structure. Firstly, using the Na I lines alone, we can constrain the position of the molecular absorbers to the position of the atomic neutrals (as seen in Na I) and compare the model with the FUSE data. In any case, we shall expect to see at most the same number of molecular components as there are atomic components. However, when the separation between component is less than 10 km s^{–1} (well below the FUSE resolution) the profile fitting of the FUSE spectra is less reliable. Secondly, we can use the Na I/Ca II ratio to diagnose which atomic component is cool and dense enough to harbor molecules. Typically, the greater the ratio the more likely the presence of dust grains and then molecules (Welty et al. 1996).

Among the possible Na I MW absorbers, two were found to match the velocity of the FUSE H₂ absorption feature: one component at +18 km s^{–1} and another component at +22 km s^{–1}. We then performed a two components analysis of the MW molecular content and find a total H₂ column density of $\log N(\text{H}_2) = 15.24 \pm 0.17$ dex, summed over the $J = 0$ –3 states (Table 8), while the rotational temperature T_{01} is about 303 K. These properties are typical of diffuse molecular clouds found in the halo as observed by Richter et al. (1999). It should be noted that our column density estimates for the individual rotational levels in the MW molecular component are somewhat larger than the estimates of Friedman et al. (2000).

There are four atomic components spanning over 30 km s^{–1} seen at the location of the LMC velocities. Imposing the 4-components solution into the FUSE data showed that the main LMC molecular absorber is associated with the atomic component at 291 km s^{–1} while less than 2 % of the H₂ is arising in the other components. We thus assume that the LMC molecular absorption lines detected in FUSE are from this single component. We find an H₂ column density of $\log N(\text{H}_2) = 19.44 \pm 0.05$ dex. With the exception of the $J = 3$ measurement, all of our estimates of the molecular hydrogen rotational levels in the LMC component are consistent with the survey by Tumlinson et al. (2002). We thus derive similar temperatures with $T_{01} \approx 57$ K and $T_{23} \approx 225$ K. The population of the rotational levels might then be used to infer the incident radiation field upon this LMC absorber.

In the following, we assume that the incident flux is responsible for the population of the rotational levels $J > 2$. This is consistent with the observation of two excitation temperatures for the H₂ component. The two temperatures are interpreted as the signatures of different processes acting together to populate the H₂ molecule from the lower levels all the way up. The levels $J = 0$ –2 are predominantly populated by collisional processes, with typi-

cal excitation temperatures below 100 K. In the Galactic disk, the population of higher rotational levels are explained by the conjugated effect of collisions, UV pumping, and formation processes (Spitzer & Zweibel 1974). However in the LMC, the radiation field is likely the main source of excitation of these higher rotational levels. Thus from the balance of the $J = 4$ level we can derive a direct estimate for the incident flux using the method developed in Wright & Morton (1979).

The basic equilibrium equation can be translated in the following manner:

$$p_4 \cdot (N_0 + N_2 + N_4) = N_{J=4} \cdot A_4 + N_4$$

where N_2 is the number of photo-excited H_2 molecules in $J = 2$, p_4 is the probability of photo-excited molecules to cascade into $J = 4$ and A_4 is the rate of radiative decay from $J=4$ to $J=2$. The number of photo-excited H_2 molecules in a given rotational level is proportional to the number of available photons multiplied by the probability of being absorbed:

$$N_4 = \int_{J=4} \left(\frac{U_\lambda c d \lambda}{h \nu} \right) \times \left(\frac{I_{\lambda 0} - I_\lambda}{I_{\lambda 0}} \right)$$

If we assume that $U_\lambda/h\nu$ is constant over the far **ultraviolet** range and equals to $(U_\lambda/h\nu)_{1000}$, then the previous equations transform into:

$$N_4 = \left(\frac{U_\lambda c}{h \nu} \right)_{1000} \times \Sigma_{J=4} W_\lambda$$

and

$$p_4 \cdot \left(\frac{U_\lambda c}{h \nu} \right)_{1000} \cdot \Sigma_{J=0,2,4} W_\lambda = N_{J=4} \cdot A_4 + \left(\frac{U_\lambda c}{h \nu} \right)_{1000} \cdot \Sigma_{J=4} W_\lambda$$

with $p_4 = 0.26$ and $A_4 = 2.76 \times 10^{-9} \text{ s}^{-1}$. The calculations of the total equivalent widths (ΣW_λ) are then computed from models of the different rotational levels based on our measurements. Solving these equations yields $U_\lambda \approx 1.9 \times 10^{-16} \text{ erg cm}^{-3} \text{ \AA}^{-1}$ which is about three times the assumed Galactic value of $\approx 7 \times 10^{-17} \text{ erg cm}^{-3} \text{ \AA}^{-1}$ (see Draine 1978; Parravano et al. 2003).

Then, with the incident flux we can estimate the distance of the cloud to the background star. The large aperture of the FUSE satellite is sampling a $30'' \times 30''$ sky area which represents about $8 \text{ pc} \times 8 \text{ pc}$ at the distance of the LMC. Since we do not see any other hot stars in the FUSE aperture, we assume that the background star is the main source of photons onto the cloud. Thus, following Bluhm & de Boer (2001), we calculate the distance using the simple cross product $\frac{I_{\text{observed}}}{I_{\text{cloud}}} = \left(\frac{d}{r_{\text{LMC}}} \right)^2$. I_{observed} is the stellar continuum intensity at 1000 \AA corrected for the extinction using the model of Cardelli, Clayton & Mathis (1989) I_{cloud} the intensity at the location of the cloud derived from our calculation, r_{LMC} is the distance to the LMC ($\approx 50 \text{ kpc}$) and d is the distance between the cloud and the background star. We find that the cloud cannot be any closer than 120 pc from Sk-67D05. This fact alone suggests that the molecular component we are looking at is probably not associated with the star formation region.

The details the MCs H_2 investigations (J levels, temperatures, radiation fields and b -values) towards each sightline are shown in Table 9.

The derived values for the HD/ H_2 ratio and the CO/ H_2 ratios are respectively $1.5 \pm 0.5 \text{ ppm}$ and $2.7 \pm 0.7 \text{ ppm}$. These values are comparable to the ones derived in the MW disk (Ferlet et al. 2000; Lacour et al. 2003 in prep). Several important questions are raised by these relatively large ratios. Firstly, the CO column density is directly influenced by the availability of C and O atoms in the gas phase; while the C and O atoms are each depleted by about 0.5 dex (Russell & Dopita 1992), the CO seems not to be depleted at all. Secondly, the lower metallicity should also result in less dust grain surfaces and then in suppressed H_2 formation. But most of the CO lines appear near the core of the H_2 absorption bands and it is usually assumed that H_2 is an efficient photo-dissociation shield for CO. The general expectation is then that the CO/ H_2 ratio would then tend to decrease when the metallicity decreases. Thirdly, the relatively small H_2 column we derive should result in a less efficient FUV-shield in this LMC cloud and a smaller CO/ H_2 ratio whatever dust content there is along the sightline.

We also detected neutral chlorine atoms which can only exist in the molecular component (see section 3.5). We find ClI/ H_2 ratio of $2.74 \pm 0.9 \text{ ppm}$ a value at least twice higher than what has been found in the Galactic disk towards HD 192639 (Sonnentrucker et al. 2002) and HD 185418 (Sonnentrucker et al. 2003). Detailed analysis of the latter lines of sight indicated that the gas was made of multiple neutral diffuse clouds. The fact that we derive a much higher ratio along a sightline where metallicity is lower by 0.5 dex with respect to the Galactic values, strongly suggests that denser molecular clumps are present towards Sk-67D05.

It is possible to get a crude estimate of the total HI column density in the LMC using the gas-to-dust ratio derived by Koorneef (1982) of $N(\text{HI})/E_{B-V} = 2 \times 10^{22} \text{ mag}^{-1} \text{ cm}^{-2}$. However, we must correct the E_{B-V} from potential MW gas contamination. Thus we calculated the MW reddening assuming $N(\text{H}_2)/E_{B-V} = 5 \times 10^{20} \text{ mag}^{-1} \text{ cm}^{-2}$ (Dufour 1982). We find that, towards Sk-67D05, the Galactic material represents only a small fraction of the total reddening of about $E_{B-V}(\text{MW}) \approx 0.01$, and thus a small fraction of the total $N(\text{HI})$ of about 10^{19} cm^{-2} . Consequently, we derive $N(\text{HI})_{\text{total}} \approx N(\text{HI})_{\text{LMC}} \approx 3 \times 10^{21} \text{ cm}^{-2}$. This HI column density is about 6 times larger than the one derived towards the same line of sight by Friedman et al. (2000). The difference is mainly due to the fact that Friedman et al. (2000) used the galactic gas-to-dust ratio which is 4 four times smaller than the LMC value (Koorneef et al. 1982). In our case, where most of the HI is originating in the LMC, this can lead to a great systematic error. Furthermore, we adopted the updated E_{B-V} as quoted in Tumlinson et al. (2002) which is 1.5 times greater than the value used by Friedman et al. (2000).

It could be argued that NaI might as well be used as a fiducial for HI with greater accuracy than the gas-to-dust ratio. Indeed, investigations of the column density correlation $N(\text{NaI})$ versus $N(\text{HI})$ by Ferlet et al. (1985) in the MW have demonstrated that NaI roughly follows HI over more than three orders of magnitude. However the abundance of sodium in the LMC gas is varying between sightlines. In the detailed investigation of Welty et al. (1999) towards SN1987A, about 20 individual LMC components were found with $\log N(\text{NaI})/N(\text{H}_{\text{total}})$ ranging from ≈ -9.0 to -9.7 dex. Here, we assume that the ratios between NaI components are reasonably linked to the ratios between HI components and we derived $N(\text{HI}) \approx 8 \times 10^{20} \text{ cm}^{-2}$ within the absorber associated with the H_2 component leading to a molecular fraction $f(\text{H}_2) = 2N(\text{H}_2)/(N(\text{HI})+2N(\text{H}_2))$ around 7 % on average over the Na components. This result together with the finding that, on average, the CO population ratio is subthermally distributed suggests that some more diffuse gas is also present along the Sk-67D05 light path.

Finally, we also measured the column density of FeII and found a value consistent with the analysis by Friedman et al. (2000): $N(\text{FeII}) = 7.0_{-1.5}^{+3.0} 10^{14} \text{ cm}^{-2}$. Note that this represents the total amount of FeII as seen in the four LMC components. Although the profile fitting made use of the four components at the same time, interpretation of FeII in each component is difficult because these are not resolved by FUSE. Fortunately, most of the FeII lines used in the profile fitting are in the optically thin regime. Hence, the total FeII we quote remains accurate. The observed abundance of Fe is then $\log [N(\text{FeII})/N(\text{H}_{\text{total}})] + 12 = 5.4$ where $N(\text{H}_{\text{total}})$ is the total amount of H atoms derived from the four absorbers using NaI. When compared with the Fe abundance in the LMC (Russell & Dopita 1992), our result implies a depletion of about 2 dex. Hence large FeII depletion occurs towards Sk-67D05 although it is not clear if FeII is depleted onto grains or in the ionized form. The fact that the CO, HD and CII analyses strongly suggest the presence of dense molecular clumps could argue in favor of depletion onto grains but the present data does not allow us to rule out the possibility that FeII might be predominantly ionized.

5.2. Sk-68D135

Sk-68D135 is a ON9.7 star located in the North of 30 Doradus region which is the largest H II region in the local group of Galaxies (Fitzpatrick & Savage 1984, Tumlinson et al. 2002). It is believed that this region requires a Lyman continuum radiation field equivalent to some 100 O5 stars to maintain its ionization. The HI data from Wayte (1990) at 8 km s^{-1} resolution reveal the presence of at least four absorbers along the sightline. Two of them arise in the MW disk and halo around +30 and +90 km s^{-1} in heliocentric velocity, while the two other are originating in the LMC at +210 and +290 km s^{-1} in heliocentric velocity. Our data however indicate the presence of 5

groups of absorbers split into 17 components and centered at (1) +30 km s^{-1} , (2) +80 km s^{-1} , (3) +160 km s^{-1} , (4) +220 km s^{-1} , and (5) +280 km s^{-1} (Table 7). The four components observed by Wayte (1990) can then be identified with group 1, 2, 4, and 5. We thus confirm that these components are in the foreground of Sk-68D135. We note also a LMC HVC located at +320 km s^{-1} showing a large CaII absorption relatively to the corresponding NaI absorption and probably indicating shocked material. Our profile fittings of the CaII and NaI VLT data are shown in Fig.4.

H_2 arising in the MW is detected in the FUSE spectrum and we identify this molecular absorber with the atomic absorber seen in NaI at 41 km s^{-1} . Not only is this absorber the strongest in NaI but it also exhibits NaI/CaII ratio of the order of 0.3 dex, typical of cold components (Welty et al. 1999). Note that adopting the complete NaI velocity structure does not improve the fit. This MW molecular component is a lot larger than the one observed towards Sk-67D05. A summary of the MW H_2 analysis is given in Table 8. We obtain $\log N(\text{H}_2) = 18.29 \pm 0.04$ dex, $T_{01} \approx 103$ K, and $T_{23} \approx 102$ K.

The investigation of the velocity structure for the molecular species observed in the LMC is a little more difficult since there are four LMC components blended within 20 km s^{-1} . The profile fitting shows that the best solution is consistent with a dominant absorber at +269 km s^{-1} along with marginal contribution from an absorber at +277 km s^{-1} (less than 1 %). We note that the absorber at +269 km s^{-1} has the largest NaI/CaII ratio of the four components and is the most likely to harbor dust grains and molecules. After profile fitting analysis assuming a single absorber, we confirm most of the H_2 measurements performed in the survey of H_2 Magellanic Clouds sightlines by Tumlinson et al. (2002). However, for the higher levels, our estimates of the mean column density are somehow different and lead us to different excitation temperatures. We find $\log N(\text{H}_2) = 19.87 \pm 0.05$ dex, $T_{01} \approx 92$ K and $T_{23} \approx 251$ K. Calculation of the incident radiation field using the same assumptions as for Sk-67D05 gives $U_\lambda \approx 2.2 \times 10^{-13} \text{ erg cm}^{-3} \text{ \AA}^{-1}$ which is several thousand times larger than the Galactic radiation field. This is a tremendously high value suggesting that the cloud is located close to the star. If we assume that the background star is the only source irradiating the cloud, we then find that the cloud is located at 5 pc from the star. A likely scenario involves a larger molecular cloud being disrupted around the star Sk-68D135. We note that the incoming radiation field we derive is similar to the ambient radiation field estimated in the 30 Dor region using CO line emissions (Bolatto et al. 1999 derived $\chi \approx 3000$). Another hint for a large radiation field comes from the observation of the strong FeIII lines at the LMC velocity. Fig. 8 compares this line to the one observed towards Sk-67D05. Unfortunately, because the line is heavily saturated it was not possible to give a quantitative measurement for the FeIII/FeII ratio. We note finally that this intense radiation field suggests that the cloud is embedded within the

30 Dor region and, therefore, may be at any distance from the background star.

That the CO and HD molecules are detected in such a harsh environment is puzzling. We actually find CO/H₂ ratio of 0.80 ppm and a HD/H₂ ratio of 1.9 ppm, values more typical of translucent ($A_V > 1$) Galactic sightlines (Rachford et al. 2002). Despite the low chlorine LMC abundance (depletion of 0.5 dex, see Russell & Dopita 1992), we find that the ClI/H₂ ratio is about 0.5 ppm again comparable to the Galactic measurements. These results, as for Sk-67D05, strongly suggest that higher density molecular clumps exist toward Sk-68D135 too.

Using the LMC gas-to-dust ratio (see section 4.1), we find that the LMC HI column density can be as high as $5 \times 10^{21} \text{ cm}^{-2}$. To derive the fraction of the molecular absorbers we assumed that the NaI ratios between components translate into HI which would lead to a HI column density of about $3 \times 10^{21} \text{ cm}^{-2}$ and a molecular fraction of 1 %. Models, however, show that such a low molecular fraction cannot be reconciliated with the detected amount of HD molecules. The photodissociation time scale for the HD molecule is given by the photodissociation rate ($2.6 \times 10^{-11} \text{ s}^{-1}$ in the Galaxy, see Le Petit et al. 2002), $T_{\text{phot}} \approx 1,500$ years. And yet this time scale should be smaller in the LMC where more photons are available. When compared to the age of the star, $T_{\text{star}} \approx 10^6$ years, this time-scale is ridiculously small and suggests that HD is locked in a dense phase where the molecules are efficiently self-shielded and where the formation routes are enhanced.

As a matter of fact, because of the location of the cloud within the 30 Dor region, and if the cloud is a remnant of a denser molecular knot, we expect the survival of CO, HD and other molecules in the core while the envelope, and all the H₂ within it, is being swept away by the shocks or the stellar winds or destroyed by photons (thus reducing the measured integrated molecular fraction), as is observed. We note also that strong shocks are in action in 30 Dor and some of the dust grains might be destroyed, releasing in the gas phase many metals. The presence of a shock along the sightline to Sk-68D135 is reinforced by the detection of the LMC HVC component at +308 km s⁻¹ with an extremely low NaI/CaII ratio of -0.5 dex.

5.3. Sk-69D246

The sightline towards Sk-69D246 has been extensively studied by Bluhm & de Boer (2001). Sk-69D246 is a WN6 star located nearby R136, at the edge of the 30 Dor complex. IUE absorption lines of SII, and MgI as well as FUSE FeII absorption lines show a velocity structure typical of most of the LMC sightlines (Danforth et al. 2002). We find three MW components around 0 km s⁻¹, a disk cloud at +40 km s⁻¹, one IVC at +80 km s⁻¹, one HVC at +130 km s⁻¹, and four LMC components at +234 km s⁻¹, +260 km s⁻¹, +280 km s⁻¹, and +290 km s⁻¹. Our high resolution VLT data of NaI and CaII make it possible to break the degeneracy associated with blended components

not seen in IUE (Fig. 5). We are indeed able to detect 18 components as described in Table 7.

The MW molecular component is associated with the component at 25 km s⁻¹ (as seen in NaI) and has the same properties as the one seen towards Sk-68D135 except for a slightly larger total H₂ column density. It is likely that both sightlines are crossing the same Galactic molecular cloud and the comparison could bring interesting limits on the variation scale across this absorber (see Sect 5.4). We find $\log N(\text{H}_2) = 18.73 \pm 0.04$ dex and calculations of the Boltzmann temperatures yield $T_{01} \approx 83$ K and $T_{23} \approx 179$ K.

The column densities for $J = 0$ to $J = 6$ in the LMC molecular component at +279 km s⁻¹ were derived by profile fitting and we noted that our fits improved noticeably when adding a second molecular component at +285 km s⁻¹ in heliocentric velocity. FUSE cannot fully resolve the two components, but we point out that a similar velocity structure was derived by Bluhm & de Boer (2001). Furthermore, ClI STIS data clearly confirm the presence of two molecular absorbers as shown in Fig. 5. For the total LMC H₂ column densities we find $\log N(\text{H}_2) = 19.66 \pm 0.04$ dex, $T_{01} \approx 70$ K and $T_{23} \approx 352$ K. The balance of the $J = 0, 2$ and 4 levels yields (see section 4.1 for details) $U_\lambda \approx 1.6 \cdot 10^{-15} \text{ erg cm}^{-3} \text{ \AA}^{-1}$. Assuming that the high J levels are mainly populated by UV-pumping and assuming that the star is the principal source of UV photons, the clouds cannot be closer than 28 pc from the background star Sk-69D246 and are possibly embedded in the 30 Dor region.

CO, HD and ClI are also detected in the LMC molecular components in relatively large amounts. The CO/H₂ ratio is of the order of 0.8 ppm, the HD/H₂ ratio is 0.9 ppm and the ClI/H₂ ratio is 0.6 ppm. *A priori*, these values are clearly unexpected in the LMC, especially in 30 Dor unless, as for the two other stars, dense clumps exist and shield these molecules from the high UV radiation field.

We derive the HI column density associated with the LMC molecular components following the two assumptions described in section 4.1: $N(\text{HI}) = 2 \cdot 10^{21} \text{ cm}^{-2}$, two times larger than the one quoted in Bluhm & de Boer (2001) who used a direct relation between SII and HI. Because the two SII components are not resolved in the IUE data and because the SII lines are saturated, the analysis of SII data is difficult and does not allow to take into account saturation effects in the core of the absorption lines. Thus, we cannot discard the fact that the HI column density may be underestimated in the work of Bluhm & de Boer (2001). The iron abundance is 5.96 leading to a depletion of 1.3 dex compared to the assumed LMC abundance (Russell & Dopita 1992). Iron seems therefore to be strongly depleted. At this point, we cannot decide whether iron was preferentially depleted onto grains or strongly ionized by the high ambient radiation field.

With the relatively high signal-to-noise of the FUSE spectrum, the LMC ClII absorption line is clearly detected at 1071 Å. At the same time, higher resolution STIS data

of the ClI line at 1347 Å are also available. We have seen that ClII is expected in the diffuse ISM where the hydrogen is atomic while ClI is associated with the molecular ISM. Adopting the Jura & York (1978) model of a single cloud made of a skin, mainly atomic, and a core, mainly molecular, one can estimate the column density $N_1(\text{H})$ of HI atoms co-located with the optically thick H_2 gas as follows: $N_1(\text{H}) = N(\text{H}_{\text{total}})(f(\text{ClI}) - f(\text{H}_2))$ where $f(\text{ClI})$ is the fraction of neutrals (ClI) among the chlorine atoms, $f(\text{H}_2)$ is the integrated molecular fraction along the sightline, $N(\text{H}_{\text{total}})$ is the integrated total column of hydrogen atoms (atomic and molecular). We estimate that the molecular fraction inside the core of the molecular component, assuming similar physical properties and chlorine depletions, is about 12%. It should be noted that this is a strong lower limit since some of the diffuse HI is possibly arising in separate pure atomic components and thus $N_1(\text{H})$ is possibly overestimated.

The LMC CI, CI*, and CI** lines are also detected towards Sk -69D246 as shown in Fig. 9. Although many absorption line multiplets are present in the FUSE range, it is difficult to isolate unblended lines. We therefore employed the STIS data around 1275 Å to perform the analysis as shown in Fig. 7, when possible. These lines were assumed to arise only in the molecular components and were fitted along with the LMC molecular hydrogen (same velocity structure, same b -values). The profile fitting analysis yields $\log N(\text{CI}) = 13.85^{+0.06}_{-0.06}$, $\log N(\text{CI}^*) = 13.72^{+0.10}_{-0.10}$, and $\log N(\text{CI}^{**}) = 13.44^{+0.05}_{-0.06}$ (see Table 6). The total fractional abundances of carbon in the excited states are $f_1 = N(\text{CI}^*)/N(\text{CI}_{\text{total}}) = 0.43 \pm 0.08$ and $f_2 = N(\text{CI}^{**})/N(\text{CI}_{\text{total}}) = 0.16 \pm 0.02$. Assuming an average radiation field of ten times the Galactic radiation field, we obtain $\log(P/k) = \log(n_{\text{H}}T)$ between 4.3 and 4.6 (Jenkins & Shaya 1979). If we assume that the carbon atoms are in the cold LMC molecular component at 72 K, then we can expect the density n_{H} to be roughly in between 300 and 600 cm^{-3} . This should be considered as a preliminary estimate since, among other simplifications, we do not take into account the multiplicity of the sightline.

Additional evidence towards the existence of a dense component comes from the detection of the $\lambda 4227$ Å CaI line at the LMC velocity. Even if the velocity structure of the line is buried within the noise of the spectrum, we can safely derive the total column density since the line is optically thin. We find $N(\text{CaI}) = 1.5^{+0.2}_{-0.2} 10^{10} \text{ cm}^{-2}$. If we assume that the ionization equilibrium pertains, the CaI/CaII ratio is a function of n_e , the radiation field and the temperature via the recombination coefficient α and the photoionization rate Γ (see section 3.6). Using $\alpha = 5.58 \times 10^{-12} \text{ cm}^3 \text{ s}^{-1}$ at $T \approx 100 \text{ K}$ and $\Gamma = 37 \times 10^{-11} \text{ s}^{-1}$ (see Péquignot & Aldrovandri 1986) multiplied by 20 to account for the larger radiation field, we find n_e ranging from 0.1 to 1 cm^{-3} . The latter values are obtained if we add the CaII component observed at 295 km s^{-1} which is probably too warm to be associated with the molecular absorbers. Compared to the previous density estimate,

this electronic density leads to an ionization fraction of 1 % at most.

5.4. AV 95

With the exception of the OVI lines studied by Howk et al. (2002), no investigation of the ISM towards AV 95 was found in the literature. Combining FUSE observations of FeII with STIS observations of SII we detect 11 atomic components. Thus, this sightline is quite typical of SMC sightlines (Welty et al. 1997; Mallouris et al. 2001) showing a number of low-ionization Galactic gas clouds or complexes spread over $\approx 65 \text{ km s}^{-1}$ (Fig. 10). Note that FeII and SII ions are tracing the neutral component as well as the HII regions. Both species seem to share the same velocity structure but exhibit different ratios between components. FeII in particular exhibits a few extra high velocity components at +169 km s^{-1} and +195 km s^{-1} (heliocentric velocities) that could correspond to shocked gas in which the grain sputtering released some of the refractory elements such as Fe into the SMC gas phase. The detailed velocity structure is summarized in Table 10.

The profile fitting of the FUSE data along with available STIS observations of ClI at $\approx 6 \text{ km s}^{-1}$ resolution is consistent with the presence of a single absorber in the MW and in the SMC with respective b -values of 1.5 km s^{-1} and 0.8 km s^{-1} . For the MW component we derive $T_{01} \approx 66 \text{ K}$, $T_{23} \approx 135 \text{ K}$, $\log N(\text{H}_2) = 18.26 \pm 0.05$, and $N(\text{ClI}) = 8.0 10^{12} \text{ cm}^{-2}$ which leads to a ClI/ H_2 ratio of 0.4 ppm. Despite the large H_2 column density we do not detect the HD molecule in this MW component.

The SMC CI, CI*, and CI** lines at 1276.48 Å, 1276.75 Å, and 1277.72 Å, available in the STIS spectra (Table 6), were first fitted along with SMC molecular hydrogen assuming common velocity structures and b -values. However, we found that these two assumptions were too strong and did not allow a proper fit of the carbon lines. Indeed, it appears that some of the carbon absorption lines arise in several components. Because our data did not allow us to reliably trace these more diffuse components, we performed a one-component fit that led to a total b -value of 5.7 km s^{-1} (about 6 times greater than the SMC H_2 adopted b -value). We note, that from the SII absorption lines detected in the FUSE range, there are many atomic diffuse components on this pathlength and some may well be cool enough to exhibit CI, CI*, and CI** lines. With these carbon lines, we inferred a range of possible H number densities for this component between 100 to 1000 cm^{-3} . Due to the SMC blending it is not possible to derive the HI content directly. One alternative way is to estimate the total sulfur column density and calculate the total hydrogen column density assuming the SMC standard abundance ($\log N(\text{SII})/N(\text{HI}) = 7.27$; see Russel & Dopita 1992) and no depletion into the grains. The total Galactic sulfur column density is hence $N(\text{S}) = 2 \times 10^{15} \text{ cm}^{-2}$ (the dominant ionization stage is SII) which leads to $N(\text{H}_{\text{total}})$ of the order of 10^{20} cm^{-2} , and $f(\text{H}_2)$ of only

3 %. The high HD/H₂ and ClI/H₂ ratios therefore suggest that denser clumps exist and are mixed with the more diffuse gas also present along the light path to AV 95 in the SMC.

The SMC molecular hydrogen is similar to the LMC ones with $T_{01} \approx 78$ K, $T_{23} \approx 245$ K, and $\log N(\text{H}_2) = 19.43 \pm 0.04$. As above, we derive the HI column density, using SII ($\log N(\text{SII})/N(\text{HI})_{\text{SMC}} = 6.6$; see Russel & Dopita 1992) and find $N(\text{HI}) \approx 10^{21} \text{ cm}^{-2}$ and $f(\text{H}_2) \approx 2.5$ %. Again, some diffuse gas must be laying along the path length in the SMC gas too. From the population of the $J = 0, 2$ and 4 levels we derive a radiation field of $1.8 \times 10^{-14} \text{ erg cm}^{-3} \text{ \AA}^{-1}$ which is 250 times greater than the average Galactic radiation field. Hence, assuming that most of this incident flux is coming from the background star, we get a lower limit on the distance between the star and the absorber of 3 pc.

The SMC CO molecule is barely detected in the FUSE spectra. We report a stringent 3σ upper limit of $\log N(\text{CO}) < 13.23$. This result is consistent with the fact that fewer oxygen atoms and fewer carbon atoms are available to form the CO molecule and that CO is more photodissociated toward this line of sight the molecular clump density being probably lower (see our previous CI results).

The SMC ClI line is clearly detected towards this star with the STIS data (1347 Å). The ClI/H₂ ratio is 0.4 ppm and translates into a depletion as low as 0.70 dex as shown in Table 9, assuming $[\text{Cl}] = 4.70$ in the SMC (Russell & Dopita 1992). However, we note that the possible presence of ClII might explain partly the low value. Indeed, the lower limit derived for the ClII ion is consistent with no depletion of chlorine atoms at all. Another test of the depletion along the sight line is given by the FeII atoms. Using HI derived from SII, we find an iron abundance of ≈ 6.4 instead of 6.84 as derived in the SMC by Russel & Dopita (1992). The relatively low iron depletion, only 0.44 dex instead of 2 dex usually reported in the MW ISM (Savage & Sembach 1996), can be due to a low dust content or is the signature of shocks, past or present (as revealed by the two SMC HVCs at $+169 \text{ km s}^{-1}$ and $+195 \text{ km s}^{-1}$). Even though the depletion is uncertain, there are clear hints of a cold medium ($T_{01} = 78$ K) with a b -value as low as 0.8 km s^{-1} (as derived from the simultaneous fit of several species) so that we cannot rule out the presence of a dense core which might harbor a D-reservoir. A D-reservoir is defined as the inner region of a cloud where all of the deuterium atoms (hydrogen atoms) are in the form of HD (H₂) molecules and where the D/H ratio thus translates into HD/2×H₂; these hypothetical places are of cosmological interest since they would allow accurate D/H measurements throughout the MW disk (Ferlet et al. 2000). The predominance of diffuse gas conditions however renders the study of this colder denser molecular gas more difficult.

Relatively large amounts of the HD molecule are detected in the SMC towards AV 95. Using both the AOD and PF techniques, we find $\log N(\text{HD}) = 13.82_{-0.18}^{+0.96}$. The large error bar is due to the possible saturation of some of

the HD lines detected in the spectra. Interestingly enough, HD/2 H₂ ranges from 1.6 ppm to 21 ppm within 1σ . The latter value, if confirmed, would correspond to the first clear detection of a D-reservoir ever (Lacour et al. 2004). Moreover, the existence of a D-reservoir is not excluded by the range of densities derived, although crudely, through the CI excited states.

5.5. Sk 159

Sk 159 is located within the Knot 1 (K1) which is rich in HII regions and is located in foreground compared with the SMC main body (De Vaucouleurs & Freeman, 1972). This region is remarkable for the homogeneity of the stellar radial velocities with a typical dispersion of 5 km s^{-1} . The investigation of this region based on Na I lines by Silvy (1996) showed that Sk 159 is located in the extreme edge of the H complex within the K1 region. The latter data are consistent with the presence of a dominant SMC atomic absorber at $+144 \text{ km s}^{-1}$ and a smaller one at $+149 \text{ km s}^{-1}$. In the FUSE data no intermediate components and no SMC HVCs are detected in Fe II. The profile fitting in the FUSE range is consistent with a single atomic component near $+150 \text{ km s}^{-1}$. However, high resolution Na I data obtained at the ESO 3.6m/CES/VLC by D. Welty (private communication) clearly show two identical components separated by approximately 5 km s^{-1} . The relative simplicity of this sightline is likely the double effect of a position of the star near the edge of the SMC and a weak foreground Galactic material. The HI radio data obtained by Wayte (1990) show two components at $+150 \text{ km s}^{-1}$ and $+190 \text{ km s}^{-1}$. The non-detection of the H component at $+190 \text{ km s}^{-1}$ in absorption (Fig. 11) shows that most of the material seen in radio is located behind the star.

The MW molecular component is quite small with $\log N(\text{H}_2) = 16.31 \pm 0.25$ and quite warm with $T_{01} \approx 153$ K. Hence, this component resembles those observed in the Galactic halo by Richter et al. (1999).

The SMC H₂ was fitted assuming a velocity structure similar to that of Na I (see D. Welty, private communication). We thus performed profile fitting of the FUSE data with this structure which led us to tentatively detect 2 molecular components: one at $+143 \text{ km s}^{-1}$ and the other one at $+152 \text{ km s}^{-1}$. We find that the integrated properties are similar to the ones observed towards AV 95 with $T_{01} \approx 87$ K, $T_{23} \approx 204$ K, and $\log N(\text{H}_2) = 19.21 \pm 0.06$. Calculation of the incident radiation field gives $3.0 \text{ erg cm}^{-3} \text{ \AA}^{-1}$ which indicates that the clouds are at least at 50 pc from Sk 159. We report on a possible weak detection of the SMC CO molecule with $\log N(\text{CO}) < 13.34$ (3σ upper limit). On the contrary, the SMC HD molecule is clearly detected in the data with $\log N(\text{HD}) = 13.85_{-0.14}^{+0.11}$ and HD/H₂ = 4.5 ppm. Thus, we obtain a lower limit to the D/H ratio of 2.3×10^{-6} inside that component. The D-reservoir does not seem to be reached. We would like to point out that this analysis is only based on FUSE data and a b -value of 2.6 km s^{-1} but higher resolution

data might unravel colder components buried in the absorption lines and then might lead to a higher HD column density.

6. Discussion

6.1. General Properties of the ISM in the MCs

In their large survey of the diffuse molecular ISM in the MCs, Tumlinson et al. (2002) have explored some of the global properties of this gas, comparing these properties to typical galactic properties, and derived a reduced H_2 formation rate, $R \approx 3 \times 10^{-18} \text{ cm}^3 \text{ s}^{-1}$ (one-third to one-tenth the Galactic rate), as well as reduced molecular fractions $f(\text{H}_2)$ of the order of 1 % (**one-tenth** the Galactic mean). These results were interpreted as the effect of suppressed H_2 formation on grains and enhanced destruction by FUV photons. The total diffuse H_2 masses were then found to be of less than 2 % of the HI mass suggesting either a small molecular content and a high star formation efficiency or the presence of substantial mass in cold, dense clouds unseen in their survey. **Although we** have only 5 stars at our disposal, we can pursue the investigation of this “pseudo” diffuse molecular ISM of the MCs with a closer look at species not investigated previously.

In this work, we have investigated three lines of sight towards the Large Magellanic Clouds and reported measurements of HD, CO, ClI and H_2 . A summary of these measurements is given in Table 9. The average HD/ H_2 ratio is 1.4 ± 0.5 ppm, the CO/ H_2 average ratio is 1.4 ± 0.5 ppm (we find 0.8 ppm when the large value towards Sk-67D05 is excluded), and the average ClI/ H_2 ratio is 1.3 ± 0.5 ppm where the quoted errors are the standard deviations. These measurements lead us to two major observations. Firstly, despite the large variation of physical conditions between the sightlines (the incident radiation field varies by 3 orders of magnitude, the total extinction varies by a factor 3 as well as the total H column densities) the standard deviation of these ratios is only of the order of 30 %. Thus, it seems that each time the HD molecule is detected in the LMC ISM we are indeed sampling the same kind of isolated cloud whose individual properties are not averaged along the pathlength, and within which the shielding is efficient enough to smooth the influence of the radiation field.

Secondly, these ratios are similar to the ones derived in the Galactic ISM. This is a bit surprising given the low total extinction towards these stars, the important incident radiation field as derived from the UV pumping, and the low abundance of carbon and chlorine atoms in the LMC. The sightline towards Sk-68D135 gives the most extreme example. We have shown (§ 4.2) that the cloud is embedded within the 30 Dor region where the radiation field is about 3,000 times greater than the typical Galactic value. Contrarily to the expectations, this sight line exhibits the largest CO/ H_2 , the largest ClI depletion, and the largest HD column density in the present sample.

Towards the SMC, we report two detections of the HD molecule, one detection of ClI, and two upper limits on the CO molecules. The ClI/ H_2 ratios is 0.4 ppm towards AV 95 well within the range of typical Galactic translucent clouds. The two lower limits that we derived for the CO/ H_2 ratio are consistent with the fact that the CO abundance is expected to be significantly smaller in the SMC (see § 5.1). The measurement of the HD molecule towards AV 95 allows for a surprisingly high HD/ H_2 ratio of 21 ppm (the largest value of the whole sample). As for CO, **such a large amount** of HD molecules is unexpected along diffuse MC’s line of sight and this observation strongly suggests that denser clumps are present and contribute significantly to the total column densities.

However, such measurements may suffer from unknown systematics and we would like to state that the profile fitting of STIS ClI data that strongly constrains the molecular components only shows saturated absorption lines for which the column densities are driven by the b -value. Our simultaneous analysis of FUSE and STIS data combining several species, however, confirms the presence of an extremely narrow SMC component (0.8 km s^{-1} of total b -value) adding weight to the suggestion that denser molecular gas is present.

Another interesting comparison of the MW ISM with the MCs ISM comes from the molecular gas-to-dust ratio. With the direct measurements of the Galactic H_2 column densities towards the MCs, we are able to correct for the reddening from the foreground Galactic material (Dufour et al. 1982; see § 4.2) and derive the intrinsic MCs’s reddening. Noteworthy is that for the five sightlines the corrections were found to be small which is consistent with the fact that our sample is biased towards low foreground Galactic column densities (see § 3.3). Finally, we find that the H_2/E_{B-V} in the LMC ranges from 1.7 to $5.2 \times 10^{20} \text{ mag}^{-1} \text{ cm}^{-2}$ in Sk-67D05 and Sk-69D246 respectively. In the SMC we derive $4.7 \times 10^{20} \text{ mag}^{-1} \text{ cm}^{-2}$ for the AV 95 line of sight and $1.7 \times 10^{20} \text{ mag}^{-1} \text{ cm}^{-2}$ for Sk159. Contrarily to the conclusion drawn in Bluhm & de Boer (2001) towards Sk-69D246, we find that these ratios compare quite well with the Galactic value from Dufour et al. (1982) of $\text{H}_2/E_{B-V} \approx 5 \times 10^{20} \text{ mag}^{-1} \text{ cm}^{-2}$ but our small sample does not allow us to make further quantitative investigations. We wish to point out that the LMC value for the $N(\text{HI})/E_{B-V}$ ratio as derived by Koorneef (1982) is $\approx 2 \times 10^{22} \text{ mag}^{-1} \text{ cm}^{-2}$ and is several times larger than in the MW disk. This is somehow consistent with smaller molecular fractions in the LMC and the fact that less dust grains (meaning less reddening) are sampled in average towards any sightline in the LMC compared to the MW.

Our investigation of the LMC and SMC ISM leads us to propose the existence of individual dense molecular structures where the translucent properties of the studied sightlines arise. This would explain the remarkable constancy of the ratios we derived despite the drastically different galactic environments. Furthermore, we propose that these clouds should be dense enough to shield effi-

ciently CO and HD despite enormous differences noted in the incident radiation fields. A preliminary estimate of the H number density using the study of atomic carbon fine structure lines observed with STIS towards Sk -69D246 and AV 95 (see Table 6) led to estimate that $n_{\text{H}} > \text{few } 100 \text{ cm}^{-3}$.

Finally, our analysis indicates that, as for the MW, the MC sightlines exhibit a mixture of diffuse and denser molecular gas. The cold molecular gas in the MCs is however more readily detected in the MC gas probably due to a lower diffuse/dense gas ratio. We indeed observe one order of magnitude less H_2 as towards typical Galactic translucent sightlines.

6.2. Molecular clumps or filaments in the MCs

It has been known for some time that the interstellar H I of the LMC is a cooler mixture of phases than in the MW. The first direct evidences were reported by Dickey et al. (1994) in their ATCA 21-cm survey within the LMC; they established that a cold atomic phase is present in the MC ISM at variance with the lack of cold phases outside of the optical boundary of the MCs (Mebold et al. 1991). Moreover, they showed that the cold atomic phase is more abundant in the LMC ISM than within the MW. A few years before, observations of the low CO luminosity of the MCs (Cohen et al. 1988; Israel et al. 1991) have been reported to be marginally consistent with the relatively large amount of atomic gas present ($\approx 2 \cdot 10^9 M_{\odot}$). The difference between observations of cold atomic phases and cold molecular phases was soon interpreted to be an effect of the phase mixing and clumpiness of the medium (Lequeux et al. 1994).

However, to date only a few hints towards a clumpy molecular phase are available. Recent ESO-SEST observations have revealed a new picture of the LMC molecular clouds with higher complexity than previously observed and molecular clumps as small as 25 pc or less, the limitation being the spatial resolution of the instrument. The SEST survey towards the LMC complex N11 by Israel et al. (2003) allows the identification of a population of dense molecular clouds ($n_{\text{H}_2} \approx 3000 \text{ cm}^{-3}$) with relatively warm temperature (60K–150K). This observation confirms the model proposed by Lequeux et al. (1994) in which the molecular complexes are seen as a collection of identical clumps of uniform density (between 10^3 – 10^5 cm^{-3}) immersed in a non uniform interclump medium with density $n_{\text{H}} \approx 100 \text{ cm}^{-3}$.

The detection of cold atomic clouds have also been reported by Kobulnicky & Dickey (1999) in absorption in the Magellanic Bridge, a 10-degree region of diffuse gas linking the main SMC body to an extended arm of the LMC. Shortly after, Lehner (2002) confirmed the existence of small molecular absorbers in the Magellanic Bridge using FUSE data. Typical densities for diffuse molecular absorbers in the MW disk (Rachford et al. 2002; Sonnentrucker et al. 2002; Sonnentrucker et al. 2003) vary

roughly in the range 1–100 cm^{-3} ; assuming that these densities hold for the Magellanic bridge and given the low column density reported by Lehner (2002) ($\log N(\text{H}_2) < 15 \text{ dex}$) we compute the sizes of these clumps in the range 10–1000 Astronomical Units (AU).

Our present observations of molecular clumps in the MCs are consistent with these later results: with typical $\log N(\text{H}_2) \approx 19 \text{ dex}$ and density $> 100 \text{ cm}^{-3}$, we derive sizes of 10^4 AU or 1/10 pc (well below the 25 pc reported by Israel et al. 2003).

The detection of CO molecules in our LMC sightlines is a strong evidence for even denser clumps for it is usually assumed that densities ranging from 1,000 to 100,000 cm^{-3} are necessary to fit the observations (Lequeux et al. 1994). Recent investigations of the H_3^+ abundances led Cecchi-Pestellini & Dalgarno (2000) to the same conclusions toward the Galactic star Cygnus OB2 no.12. Our observations favor as well the existence of dense clumps embedded in a tenuous interclump medium. Not only do we find that the CO/ H_2 ratio is relatively high, indicative of denser gas, but also that the investigation of the rotational levels of the CO molecules in the LMC targets leads to $\langle T_{\text{ex}}(\text{CO}) \rangle \approx 9 \text{ K}$ typical of subthermal excitation occurring in cold clouds (see Fig 12).

In fact, if we adopt the model of clumpy diffuse ISM derived by Cecchi-Pestellini & Dalgarno (2002) we find densities of the order of 10^4 cm^{-3} . At face value, this leads to extremely small clump with sizes of 10^3 AU , 10^2 AU , and smaller (the solar system is about 150 AU). However, several objections can be raised against the existence of such small molecular blobs. First, we can compare the probability for such an absorber to cross the light path to a MCs bright star with the actual covering factor. Assuming that the total molecular phase hidden in these blobs is of the order of $10^7 M_{\odot}$ ($10^9 M_{\odot}$ in cold atomic phase \times a molecular fraction of 1%, see Dickey et al. 1999 and Tumlinson et al. 2002) over a $1 \text{ kpc} \times 1 \text{ kpc}$ sky area (dimensions of the 30 Dor region), assuming that the blobs are randomly distributed in volume, then, knowing the radius (0.05 pc) and the mass of each blob ($\approx 0.1 M_{\odot}$ with $n_{\text{H}} = 10^4 \text{ cm}^{-3}$) we infer a crude covering factor of the order of 40 %. This is inconsistent with our observation that 3 LMC sightlines out of 55 ($\approx 5 \%$) and 2 out of 26 SMC sightlines ($\approx 8 \%$) are crossing these clumps (even taking into account a handful of eventual misdetections; see § 2.1). It should be noted, however, that in the above picture, it is assumed that most of the molecular mass resides in cold, dense clumps which is not demonstrated. Second, if we assume that these blobs are roughly spherical then the dimensions we derive are ill-defined or should be considered only lower limits to the total radius. In effect, there is a larger probability to cross the outskirts than the core of such a clump and the frequency of core-crossing sightlines remains, by nature, a hidden parameter. Anyhow, this later scenario fails also to predict the observed similarities between sightlines (for instance, all the absorbers have total H_2 column densities within a factor of two).

Filementary structures are, then, an interesting alternative. A small fraction of the molecular gas condensed in such structures could result in a relatively large covering factor if they are preferentially found nearby the stars (this is the case for all our targets except for Sk-67D05). At the same time they provide a natural explanation for the about constant total H₂ content since a deviation of 60 degrees from a normal incidence upon a filament results in a mere factor two difference in the total crossing path.

The question of the origin of these small structures is out of the scope of this paper. Whether their formation is triggered by stellar formation processes or whether these clouds are small evaporating pieces of a parent body cannot be answered yet. Finally, we note that resilient molecular structures have to be present within star forming regions of the MCs and our conclusion follows the one by Dickey et al. (1994) who reported a clear correlation between the cold atomic phase and the star forming regions within the LMC.

6.3. A possible lower limit for the D/H ratio in the SMC of 1.1×10^{-5} ?

Measurements of the atomic D/H ratio have been performed in different astrophysical sites, in particular within Damped Lyman Alpha (DLAs) systems observed towards high redshift quasar absorbers. The DLAs have generally a few % solar metallicity and are the best candidates to investigate the primordial abundance of deuterium. However, these measurements are difficult to achieve and suffer from several systematics, one of which being the confusion due to the blend **between** several HI absorbers along crowded lines of sight (Lemoine et al. 1999). At this time, definitive conclusions are out of reach although a trend towards $D/H_{\text{primordial}} \approx 3.5 \times 10^{-5}$ emerges (Kirkman et al. 2001; see for a review Lemoine et al. 1999). The D/H ratio has also been thoroughly investigated in the Local ISM (see the review by Moos et al. 2002) with the FUSE satellite. These studies indicate that the deuterium abundance is about constant within 100 pc at 1.5×10^{-5} with a standard deviation of 20 %. This value is regarded as representative of the current D/H ratio. Whether this abundance is representative of the current ISM or whether the LISM has peculiar abundances is still a question of debate. At rare occasions, the D/H ratio has been measured in the MW along pathlength greater than 1 kpc and was consistently found smaller than the LISM value around 0.8×10^{-5} (Hoopes et al. 2003; Hébrard & Moos 2003).

The determination of the deuterium abundance in the MCs is of great importance to better understand the chemical evolution of the Universe through D/H from the Big Bang Nucleosynthesis (BBN) to the current ISM. D/H in the SMC, with two tenths of solar metallicity, would allow to have one measurement in the time range between the DLAs formation and the current MW ISM. Unfortunately, because the deuterium lines appears next

to the HI lines, the DI lines are usually severely blended by the large galactic HI lines at the SMC velocity.

Another way of investigating the D/H ratio consists in studying the deuterated species present in the MC ISM such as DCO⁺, DCN, ND₃ or HD. However, apart from the case of the HD molecule, the model used to interpret the fractionation of the deuterium atoms are far from being reliable. For instance, recent observations of the ratio NH₃/ND₃ is in strong disagreement with the models, ND₃ is found overabundant by a factor 10,000 (van der Tak et al. 2002). Thus, although one D/H measurement (around 1.5×10^{-5}) has been attempted via DCO⁺ and DCN by Chin et al. (1996) in the SMC, the best probe for the deuterium abundance in the MCs still remains the HD/H₂ ratio provided there are molecular cores where the deuterium atoms are simply in the form of the HD molecules. In these so-called D-reservoirs $HD/H_2 = 2 \times D/H$.

At present, from all the extragalactic FUSE targets observed to date AV 95 is the most promising for that purpose. With a HD/H₂ ratio possibly as high as 2.2×10^{-5} , we can derive D/H of the order of 1.1×10^{-5} that is slightly smaller than the value found in the LISM but larger than the value measured towards the two extended MW sightlines HD 191877 and HD 195695 (Hoopes et al. 2003) with D/H ratios of 0.78×10^{-5} and 0.85×10^{-5} respectively. For now, unfortunately, the analysis of the HD/H₂ ratio towards AV 95 with the existing FUSE data does not allow us to exclude a much more reduced value of HD/H₂ of 2×10^{-6} . In order to further investigate this interesting sightline higher resolution data are mandatory. Such high resolution data could be obtained in the optical by a tracer of H₂ and HD (Lacour et al. 2004) such as CH at 4300 Å. This observational effort would not only lead to the first clear detection of a deuterium reservoir but also help to constrain cosmological models predicting the deuterium evolution as a function of metallicity.

6.4. Molecular filaments detected in the MW

LMC and SMC sightlines are especially well suited for the investigation of spatial variations in the ISM of our Galaxy (Ferlet 1999). Since the angular distance between MC background stars is much reduced compared with the MW stars, they can be used as probe of degree-scale structures in the MW. Two of the stars of our mini-survey are close enough to allow for a test of these fine structures: Sk-68D135 and Sk-69D246 are within 30' from each other. The same NaI component is detected around +25 km s⁻¹ with similar *b*-values for both stars.

At 1 kpc, 30' would correspond to a linear distance of 10 pc. We have seen that both clouds have kinetic temperatures around 100 K, as deduced from T_{01} , with molecular hydrogen column densities around $\log N(\text{H}_2) \approx 18$. Then, assuming that these absorbers are within the thick disk which extends at ± 250 pc from the Galactic plane, the corresponding absorber scale is of the order of 2.5 pc or smaller in the direction perpendicular to the sightline. It

is reasonable to assume that we are indeed observing the same molecular structure.

In the case of Sk –69D246, the carbon lines detected in the STIS spectrum give a diagnostic of the density within the absorber from 60 to 600 atoms cm^{-3} (Table 6). Then, from the estimation of the total H_2 column density, we have a rough estimate of the length of the crossed medium in the direction of the sightline which is about 10^3 to 10^4 AU or 0.1 to 0.01 pc.

It is clear from these calculations that the molecular structure observed is extremely filamentary with a ratio width/length probably in between 0.4 % and 4 %.

Filamentary structures have been observed for the first time in the Pleiades nebulosity (Osterbrock 1959) in optical data and later in radio via the polarization of the H I lines emitted in the Crab Nebula (Wright 1970). Today, such structures are commonly observed in the MW or even in the extragalactic ISM on scales from tens to hundreds of parsecs (Houllahan & Scalo 1985; Kulkarni & Heiles 1988, Curry 2000). Smaller scales have tentatively been identified in HI towards high-velocity pulsars and extragalactic radio sources (Frail et al. 1994; Faison et al. 1998) down to the AU scale. Confirmation is brought by recent spectroscopic investigations of the Galactic ISM gas (see Lauroesch, Meyer & Blades 2000; Richter, Sembach & Howk 2003, Rollinde et al. 2003) although it is not clear yet whether such structures, called TSAS for Tiny-Scale Atomic Structures, are filamentary. Our present observations add weight, from the observational point of view, to the existence and the filamentary nature of the TSMS: Tiny-Scale Molecular Structures.

7. Conclusions

1. We have studied the sightlines towards three LMC bright stars: Sk –67D05, Sk –68D135, and Sk –69D246. The combination of ground-based observations (VLT) along with archival data from UV satellites (FUSE, STIS) makes it possible to investigate H_2 , CO, HD, CII, CIII, CI, CI*, CI**, NaI, CaI, CaII, FeII, and SII. We also report on the investigation of two SMC sightlines with the help of FUSE and STIS data. With the exception of NaI, CaI, and CaII, we have obtained measurements or upper limits on all the species observed towards the LMC targets.
2. In the LMC we find $\langle \text{HD}/\text{H}_2 \rangle = 1.4$ ppm, $\langle \text{CO}/\text{H}_2 \rangle = 1.4$ ppm (0.8 ppm when excluding the large value obtained toward Sk –67D05), and $\langle \text{CII}/\text{H}_2 \rangle = 1.3$ ppm. After correcting for the MW reddening we also derive $\langle N(\text{H}_2)/E_{B-V} \rangle = 3.5 \pm 1.8 \times 10^{20} \text{ mag}^{-1} \text{ cm}^{-2}$. The analysis of the rotational levels of the H_2 molecules gives the kinetic temperature of the crossed molecular gas about $\langle T_{01} \rangle \approx 70$ K. All these values are similar to values obtained in the MW disk and seem a bit surprising in the LMC where the radiation field is 5 to 3,000 times more intense than in the MW disk and the metallicity down by a factor 2. We suggest that these observations are consistent with the exis-

tence of cold, dense molecular structures embedded in the diffuse gas.

3. In the SMC, we find $\langle N(\text{H}_2)/E_{B-V} \rangle = 4.7$ and $1.7 \times 10^{20} \text{ mag}^{-1} \text{ cm}^{-2}$ for AV 95 and Sk 159 respectively. The sightline towards AV 95 in particular shows unexpectedly large HD/ H_2 (21 ppm) ratio. We tentatively conclude that a D-reservoir is detected that can give access to a direct measure of the D/H in the SMC. However, more observations are needed, with better S/N and higher resolution, in order to confirm our analysis.
4. The detailed analysis of the excited states of the carbon atoms gives an interesting diagnostic of the H number density along the sightlines towards Sk –69D246 and AV 95. For both stars we find that the density is greater than 10^2 cm^{-3} in the LMC molecular components. This leads to clump sizes (or filament) of the order of 0.1 pc. Indeed, we note that there are hints for an even denser medium and sizes of the order of 10^2 AU (≈ 0.001 pc). We reached the same conclusions for the Galactic molecular component sampled by the Sk –68D135 and the Sk –69D246 sightlines. We argue that this component probably corresponds to a sheet-like structure such as the ones recently inferred in the Galactic halo (Richter et al. 2003). More quantitative conclusions are to be given in the following paper based on the chemical model of Le Petit et al. (2002).

Acknowledgements. This work was partially done using the procedure *Owens.f* developed by M. Lemoine and the FUSE french team. It is our great pleasure to thank Eric Maurice for bringing to our attention the PhD thesis of Jocelyne Silvy and D. Welty for sharing with us some of his VLT data towards Sk 159. We gratefully acknowledge the referee, K.S. de Boer, for his helpful comments.

References

- Abgrall, H., Roueff, E., Launay, F., Roncin, J. Y., & Subtil, J. L. 1993a, A&AS, 101, 273
- Abgrall, H., Roueff, E., Launay, F., Roncin, J. Y., & Subtil, J. L. 1993b, A&AS, 101, 323
- Abgrall, H., Roueff, E., & Drira, I. 2000, A&AS, 141, 297
- Abgrall, H., Roueff, E. 2003 in preparation
- Ballester, P., Grosbol, P., Banse, K., Disaro, A., Dorigo, D., Modigliani, A., Pizarro de la Iglesia, J. A., & Boitquin, O. 2000, Proc. SPIE, 4010, 246
- Bertin, P., Lallement, R., Ferlet, R., & Vidal-Madjar, A. 1993, A&A, 278, 549
- Bluhm, H. & de Boer, K. S. 2001, A&A, 379, 82
- Boehringer, H. & Hartquist, T. W. 1987, MNRAS, 228, 915
- Bolatto, A. D., Jackson, J. M., & Ingalls, J. G. 1999, ApJ, 513, 275
- Cardelli, J. A., Clayton, G. C., & Mathis, J. S. 1989, ApJ, 345, 245
- Cecchi-Pestellini, C. & Dalgarno, A. 2002, MNRAS, 331, L31
- Cecchi-Pestellini, C. & Dalgarno, A. 2000, MNRAS, 313, L6
- Chin, Y.-N., Henkel, C., Millar, T. J., Whiteoak, J. B., & Mauersberger, R. 1996, A&A, 312, L33

- Chu, Y.-H., Wakker, B., Mac Low, M.-M., & Garcia-Segura, G. 1994, *AJ*, 108, 1696
- Cohen, R. S., Dame, T. M., Garay, G., Montani, J., Rubio, M., & Thaddeus, P. 1988, *ApJ*, 331, L95
- Curry, C. L. 2000, *ApJ*, 541, 831
- Curry, C. L. 2002, *ApJ*, 576, 849
- Danforth, C. W., Howk, J. C., Fullerton, A. W., Blair, W. P., & Sembach, K. R. 2002, *ApJS*, 139, 81
- de Boer, K. S., Koornneef, J., & Savage, B. D. 1980, *ApJ*, 236, 769
- Dekker, H., D'Odorico, S., Kaufer, A., Delabre, B., & Kotzłowski, H. 2000, *Proc. SPIE*, 4008, 534
- Dickey, J. M., Mebold, U., Marx, M., Amy, S., Haynes, R. F., & Wilson, W. 1994, *A&A*, 289, 357
- Diplas, A. & Savage, B. D. 1994, *ApJ*, 427, 274
- de Vaucouleurs, G. & Freeman, K. C. 1972, *Vistas in Astronomy*, 14, 163 B. D. 1994, *ApJ*, 427, 274
- Draine, B. T. 1978, *ApJS*, 36, 595
- Dufour, R. J., Shields, G. A., & Talbot, R. J. 1982, *ApJ*, 252, 461
- Ehrenfreund, P. et al. 2002, *ApJ*, 576, L117
- Faison, M. D., Goss, W. M., Diamond, P. J., & Taylor, G. B. 1998, *AJ*, 116, 2916
- Ferlet, R., Vidal-Madjar, A., & Gry, C. 1985, *ApJ*, 298, 838
- Ferlet, R. 1999, *A&A Rev.*, 9, 153
- Ferlet, R. et al. 2000, *ApJ*, 538, L69
- Fitzpatrick, E. L. & Savage, B. D. 1984, *ApJ*, 279, 578
- Frail, D. A., Weisberg, J. M., Cordes, J. M., & Mathers, C. 1994, *ApJ*, 436, 144
- Friedman, S. D. et al. 2000, *ApJ*, 538, L39
- Garay, G., Johansson, L. E. B., Nyman, L.-Å., Booth, R. S., Israel, F. P., Kutner, M. L., Lequeux, J., & Rubio, M. 2002, *A&A*, 389, 977
- Garnett, D. R., Shields, G. A., Peimbert, M., Torres-Peimbert, S., Skillman, E. D., Dufour, R. J., Terlevich, E., & Terlevich, R. J. 1999, *ApJ*, 513, 168
- Hébrard, G. et al. 2002, *ApJS*, 140, 103
- Hébrard, G. & Moos, H. W. 2003, *ApJ*, 599, 297
- Herbig, G. H. 1995, *ARA&A*, 33, 19
- Hoopes, C. G., Sembach, K. R., Hébrard, G., Moos, H. W., & Knauth, D. C. 2003, *ApJ*, 586, 1094
- Houllahan, P. & Scalzo, J. M. 1985, *BAAS*, 17, 835
- Howk, J. C., Savage, B. D., Sembach, K. R., & Hoopes, C. G. 2002, *ApJ*, 572, 264
- Israel, F. P. 1991, *IAU Symp.* 146: Dynamics of Galaxies and Their Molecular Cloud Distributions, 146, 13
- Israel, F. P. et al. 2003, *A&A*, 401, 99
- Jenkins, E. B. & Shaya, E. J. 1979, *ApJ*, 231, 55
- Jenkins, E. B., Savage, B. D., & Spitzer, L. 1986, *ApJ*, 301, 355
- Jenkins, E. B. & Tripp, T. M. 2001, *ApJS*, 137, 297
- Jura, M. 1974, *ApJ*, 190, L33
- Jura, M. & York, D. G. 1978, *ApJ*, 219, 861
- Kimble, R. A. et al. 1998, *Proc. SPIE*, 3356, 188
- Kirkman, D. et al. 2001, *ApJ*, 559, 23
- Kobulnicky, H. A. & Dickey, J. M. 1999, *AJ*, 117, 908
- Koornneef, J. 1982, *A&A*, 107, 247
- Kulkarni, S. R. & Heiles, C. 1988, *Galactic and Extragalactic Radio Astronomy*, 95
- Lauroesch, J. T., Meyer, D. M., & Blades, J. C. 2000, *ApJ*, 543, L43
- Lacour, S., Le Petit, F., Sonnentrucker, P., André, M., Désert, J. M., Ferlet, R., & Roueff, 2004 in preparation
- Lehner, N. 2002, *ApJ*, 578, 126
- Lehner, N., Gry, C., Sembach, K. R., Hébrard, G., Chayer, P., Moos, H. W., Howk, J. C., & Désert, J.-M. 2002, *ApJS*, 140, 81
- Lemoine, M. et al. 1999, *New Astronomy*, 4, 231
- Lemoine, M. et al. 2002, *ApJS*, 140, 67
- Le Petit, F., Roueff, E., & Le Bourlot, J. 2002, *A&A*, 390, 369
- Lequeux, J., Le Bourlot, J., Des Forets, G. P., Roueff, E., Boulanger, F., & Rubio, M. 1994, *A&A*, 292, 371
- Mallouris, C. et al. 2001, *ApJ*, 558, 133
- McKee, C. F. & Ostriker, J. P. 1977, *ApJ*, 218, 148
- Mebold, U., Herbstmeier, U., Kalberla, P. M. W., Greisen, E. W., Wilson, W., & Haynes, R. F. 1991, *A&A*, 251, L1
- Moos, H. W. et al. 2000, *ApJ*, 538, L1
- Morton, D. C. & Noreau, L. 1994, *ApJS*, 95, 301
- Neubig, M. M. S. & Bruhweiler, F. C. 1997, *AJ*, 114, 1951
- Osterbrock, D. E. 1959, *PASP*, 71, 23
- Parravano, A., Hollenbach, D. J., & McKee, C. F. 2003, *ApJ*, 584, 797
- Péquignot, D. & Aldrovandi, S. M. V. 1986, *A&A*, 161, 169
- Pfenniger, D., Combes, F., & Martinet, L. 1994, *A&A*, 285, 79
- Pottasch, S. R. 1972, *A&A*, 20, 245
- Rachford, B. L. et al. 2001, *ApJ*, 555, 839
- Rachford, B. L. et al. 2002, *ApJ*, 577, 221
- Richter, P., de Boer, K. S., Widmann, H., Kappelman, N., Gringel, W., Grewing, M., & Barnstedt, J. 1999, *Nature*, 402, 386
- Richter, P., Sembach, K. R., & Howk, J. C. 2003, *A&A*, 405, 1013
- Rollinde, E., Boissé, P., Federman, S. R., & Pan, K. 2003, *A&A*, 401, 215
- Roueff, E. & Zeppen, C. J. 2000, *A&AS*, 142, 475
- Russell, S. C. & Dopita, M. A. 1992, *ApJ*, 384, 508
- Sahnow, D. J. et al. 2000, *ApJ*, 538, L7
- Savage, B. D. & de Boer, K. S. 1981, *ApJ*, 243, 460
- Savage, B. D. & Sembach, K. R. 1991, *ApJ*, 379, 245
- Savage, C., Apponi, A. J., Ziurys, L. M., & Wyckoff, S. 2002, *ApJ*, 578, 211
- Schectman, R. M., Federman, S. R., Beideck, D. J., & Ellis, D. J. 1993, *ApJ*, 406, 735
- Schramm, D. N. & Turner, M. S. 1998, *Reviews of Modern Physics*, 70, 303
- Sembach, K. R. & Savage, B. D. 1992, *ApJS*, 83, 147
- Silvy, J. 1996, PhD Université de Marseille
- Snow, T. P. & Cohen, J. G. 1974, *ApJ*, 194, 313
- Snowden, S. L. & Petre, R. 1994, *ApJ*, 436, L123
- Songaila, A. 1981, *ApJ*, 248, 945
- Sonneborn, G. et al. 2002, *ApJS*, 140, 51
- Sonnentrucker, P., Friedman, S. D., Welty, D. E., York, D. G., & Snow, T. P. 2002, *ApJ*, 576, 241
- Sonnentrucker, P., Friedman, S. D., Welty, D. E., York, D. G., & Snow, T. P. 2003, *ApJ*, 596, 350
- Spitzer, L. J. & Cochran, W. D. 1973, *ApJ*, 186, L23
- Spitzer, L. J. & Zweibel, E. G. 1974, *ApJ*, 191, L127
- Tumlinson, J. et al. 2002, *ApJ*, 566, 857
- van der Tak, F. F. S., Schilke, P., Müller, H. S. P., Lis, D. C., Phillips, T. G., Gerin, M., & Roueff, E. 2002, *A&A*, 388, L53
- Varshalovich, D. A., Ivanchik, A. V., Petitjean, P., Srianand, R., & Ledoux, C. 2001, *Astronomy Letters*, 27, 683
- Vidal-Madjar, A., Andreani, P., Cristiani, S., Ferlet, R., Lanz, T., & Vladilo, G. 1987, *A&A*, 177, L17
- Vladilo, G., Molaro, P., Monai, S., D'Odorico, S., Ferlet, R., Vidal-Madjar, A. V., & Dennefeld, M. 1993, *A&A*, 274, 37

- Wayte, S. R. 1990, *ApJ*, 355, 473
- Welty, D. E., Morton, D. C., & Hobbs, L. M. 1996, *ApJS*, 106, 533
- Welty, D. E., Lauroesch, J. T., Blades, J. C., Hobbs, L. M., & York, D. G. 1997, *ApJ*, 489, 672
- Welty, D. E., Frisch, P. C., Sonneborn, G., & York, D. G. 1999, *ApJ*, 512, 636
- Welty, D. E. & Hobbs, L. M. 2001, *ApJS*, 133, 345
- Wood, B. E., Linsky, J. L., Hébrard, G., Vidal-Madjar, A., Lemoine, M., Moos, H. W., Sembach, K. R., & Jenkins, E. B. 2002, *ApJS*, 140, 91
- Woodgate, B. E. et al. 1998, *PASP*, 110, 1183
- Woosley, S. E. & Weaver, T. A. 1995, *ApJS*, 101, 181
- Wright, M. C. H. 1970, *MNRAS*, 150, 271
- Wright, E. L. & Morton, D. C. 1979, *ApJ*, 227, 483
-

Table 1. Lines of sight properties and references.

| LMC/SMC stars | R.A. J2000 | Decl. J2000 | Spectral Type | $E_{(B-V)}$ ^a | References |
|---------------|---------------|----------------|------------------|--------------------------|------------|
| Sk-67D05 | 4 50 18.96 | -67 39 37.90 | O9.7Ib | 0.16 | 1, 2 |
| Sk-68D135 | 5 37 48.60 | -68 55 8.00 | ON9.7Ia+ | 0.27 | 1, 3 |
| Sk-69D246 | 5 38 53.50 | -69 2 0.70 | WN6h | 0.10 | 1, 4 |
| AV 95 | 0 51 21.54 | -72 44 12.90 | O7 III | 0.06 | 1 |
| Sk 159 | 1 15 58.84 | -73 21 24.10 | B0.5 Iaw | 0.09 | 1 |

^a Total color excess (MW+LMC)¹ Tumlinson et al. (2002),² Friedman et al. (2000),³ Ehrenfreund et al. (2002),⁴ Bluhm & DeBoer (2002)**Table 2.** Log of FUSE observations ^a.

| LMC/SMC stars | Dataset | Date | Exposure time ^b Ksecs | S/N per pixel |
|---------------|----------|------------|-------------------------------------|------------------|
| Sk-67D05 | P1030703 | 2000-10-07 | 3.5 | 5 |
| | P1030704 | 2000-10-04 | 4.0 | 6 |
| Sk-68D135 | P1173901 | 2000-02-12 | 6.8 | 5 |
| Sk-69D246 | P1031802 | 1999-12-16 | 22.1 | 9 |
| AV 95 | P1150404 | 2000-05-31 | 13.8 | 7 |
| Sk 159 | P1030501 | 2000-10-11 | 6.9 | 5 |

^a All these targets have been observed in Time-Tagged (TTAG)mode through the large aperture (LWRS)^b After sorting for bad data**Table 3.** Log of VLT/UVES observations obtained on the 27th May 2003*.

| Begin (UT) | Object | Exposure time (s) | Air Mass Start | Air Mass End | Setup |
|---------------|-----------|----------------------|----------------------|--------------------|-------------------|
| 23:26 | Sk-69D246 | 1200 | 1.69 | 1.76 | Standard Dichroic |
| 23:50 | Sk-68D135 | 1200 | 1.78 | 1.86 | Standard Dichroic |
| 00:16 | Sk-67D05 | 1200 | 2.14 | 2.28 | Standard Dichroic |
| 00:42 | Sk-68D135 | 489 | 2.02 | 2.06 | Non Standard Red |
| 01:07 | Sk-69D246 | 900 | 2.16 | 2.27 | Non Standard Red |
| 01:29 | Sk-67D05 | 513 | 2.79 | 2.89 | Non Standard Red |

* observations collected at the European Southern Observatory, Paranal, Chile [ESO VLT 69.A-0123(A)].

Table 4. Log of HST/STIS observations.

| Star | ID | Date | Exposure (s) | Aperture |
|-----------|-----------|------------|--------------|---------------|
| Sk-69D246 | 06LZ12010 | 2002-11-13 | 1200 | 0''.2 × 0''.2 |
| AV 95 | 04WR17010 | 1999-05-16 | 2448 | 0''.2 × 0''.2 |
| | 04WR17020 | 1999-05-16 | 3168 | 0''.2 × 0''.2 |

Table 5. Summary of lines used in this work.

| Species | Wavelength (Å) | f -value | Dataset |
|--------------------------|-------------------|------------------------|---------|
| CI | 1276.4822 | 0.449×10^{-2} | STIS |
| CI | 1277.2452 | 0.932×10^{-1} | STIS |
| CI* | 1276.7498 | 0.252×10^{-2} | STIS |
| CI* | 1277.2827 | 0.705×10^{-1} | STIS |
| CI* | 1277.5131 | 0.223×10^{-1} | STIS |
| CI* | 1279.0562 | 0.736×10^{-3} | STIS |
| CI* | 1279.8907 | 0.126×10^{-1} | STIS |
| CI** | 1277.1899 | 0.273×10^{-3} | STIS |
| CI** | 1277.5500 | 0.791×10^{-1} | STIS |
| CI** | 1277.7233 | 0.155×10^{-1} | STIS |
| CI** | 1277.9539 | 0.817×10^{-3} | STIS |
| CI** | 1279.2290 | 0.378×10^{-2} | STIS |
| CI** | 1279.4980 | 0.199×10^{-3} | STIS |
| CaI | 4227.9180 | 0.175×10^{-1} | VLT |
| CaII | 3934.7750 | 0.629×10^0 | VLT |
| CaII | 3969.5901 | 0.312×10^0 | VLT |
| ClI | 1088.0590 | 0.810×10^{-1} | FUSE |
| ClI | 1347.2396 | 0.153×10^0 | STIS |
| ClII | 1071.035 | 0.150×10^{-1} | FUSE |
| FeII | 1125.4478 | 0.160×10^{-1} | FUSE |
| FeII | 1127.0984 | 0.282×10^{-2} | FUSE |
| FeII | 1143.2260 | 0.177×10^{-1} | FUSE |
| FeIII | 1122.5240 | 0.544×10^{-1} | FUSE |
| NaI | 5891.5833 | 0.641×10^0 | VLT |
| NaI | 5897.5581 | 0.320×10^0 | VLT |
| HD Lyman (V14-0, $J=0$) | 959.8174 | 0.147×10^{-1} | FUSE |
| HD Werner (V0-0, $J=0$) | 1007.2830 | 0.325×10^{-1} | FUSE |
| HD Lyman (V8-0, $J=0$) | 1011.4570 | 0.262×10^{-1} | FUSE |
| HD Lyman (V5-0, $J=0$) | 1042.8480 | 0.206×10^{-1} | FUSE |
| HD Lyman (V3-0, $J=0$) | 1066.2710 | 0.115×10^{-1} | FUSE |
| CO (C-X, $J=0$) | 1087.8669 | 0.619×10^{-1} | FUSE |
| CO (C-X, $J=1$) | 1087.9590 | 0.206×10^{-1} | FUSE |
| CO (C-X, $J=1$) | 1087.8209 | 0.413×10^{-1} | FUSE |
| CO (C-X, $J=2$) | 1088.0040 | 0.247×10^{-1} | FUSE |
| CO (C-X, $J=2$) | 1087.7739 | 0.371×10^{-1} | FUSE |
| CO (C-X, $J=3$) | 1088.0480 | 0.265×10^{-1} | FUSE |
| CO (C-X, $J=3$) | 1087.7260 | 0.354×10^{-1} | FUSE |
| CO (C-X, $J=4$) | 1088.0919 | 0.275×10^{-1} | FUSE |
| CO (C-X, $J=4$) | 1087.6780 | 0.344×10^{-1} | FUSE |

Table 6. Logarithmic column densities of carbon for two sightlines.

| | Sk-69D246 | AV 95 |
|--------------------------|-------------------------|-------------------------|
| | Galaxy | Galaxy |
| CI | $13.40^{+0.08}_{-0.10}$ | $13.64^{+0.60}_{-0.60}$ |
| CI* | $13.16^{+0.08}_{-0.18}$ | $13.37^{+0.25}_{-0.25}$ |
| CI** | $12.95^{+0.15}_{-0.12}$ | $12.78^{+0.22}_{-0.18}$ |
| f_1^a | 0.30 ± 0.15 | 0.32 ± 0.26 |
| f_2^a | 0.18 ± 0.10 | 0.08 ± 0.24 |
| n_H range ^b | [60...600] | [30...600] |
| | LMC | SMC |
| CI | $13.85^{+0.06}_{-0.06}$ | $12.90^{+0.27}_{-0.20}$ |
| CI* | $13.72^{+0.10}_{-0.10}$ | $12.95^{+0.25}_{-0.18}$ |
| CI** | $13.44^{+0.05}_{-0.06}$ | $12.70^{+0.20}_{-0.40}$ |
| f_1^a | 0.35 ± 0.07 | 0.41 ± 0.07 |
| f_2^a | 0.18 ± 0.10 | 0.23 ± 0.28 |
| n_H range ^c | [300...600] | [100...800] |

^a $f_1 = N(\text{CI}^*)/N(\text{CI}_{\text{total}})$ and $f_2 = N(\text{CI}^{**})/N(\text{CI}_{\text{total}})$.

^b The total density is derived from the model of Jenkins & Shaya (1979) assuming the average Galactic radiation field.

^c Same as ^b but assuming 10 times the average Galactic radiation field.

Table 7. Ca II and Na I component parameters towards the LMC.

| Star | Comp | V_{hel} | N_{10} | b | V_{hel} | N_{11} | b |
|------------|------|------------------|-------------------------|--------------------|------------------|-------------------------|--------------------|
| | | Ca II | 10^{10}cm^{-2} | km s^{-1} | Na I | 10^{11}cm^{-2} | km s^{-1} |
| Sk –67D05 | 1 | -11 | 35.5 | 11.2 | | | |
| | 2 | 0 | 8.6 | 3.8 | | | |
| | 3 | 6 | 31.5 | 2.3 | 6 | 0.7 | 0.4 |
| | 4 | 9 | 17.8 | 1.7 | | | |
| | 5 | | | | 15 | 3.2 | 5.8 |
| | 6 | 18 | 56.8 | 4.8 | 18 | 1.2 | 2.2 |
| | 7 | | | | 22 | 2.6 | 0.8 |
| | 8 | 77 | 4.8 | 2.3 | | | |
| | 9 | 144 | 6.2 | 3.0 | | | |
| | 10 | 256 | 6.5 | 0.7 | | | |
| | 11 | 266 | 5.3 | 1.4 | 269 | 0.9 | 2.9 |
| | 12 | 275 | 54.5 | 3.0 | 274 | 3.5 | 1.4 |
| | 13 | 284 | 62.8 | 3.5 | 284 | 18.0 | 1.6 |
| | 14 | 288 | 13.9 | 3.1 | 291 | 8.5 | 1.2 |
| Sk –68D135 | 1 | 15 | 71.6 | 10.4 | 19 | 1.7 | 0.5 |
| | 2 | 23 | 46.2 | 1.6 | 20 | 3.9 | 6.4 |
| | 3 | | | | 27 | 12.2 | 1.8 |
| | 4 | 63 | 146.0 | 8.5 | | | |
| | 5 | 76 | 26.2 | 2.9 | | | |
| | 6 | | | | 84 | 1.2 | 12.7 |
| | 7 | 154 | 23.0 | 4.3 | | | |
| | 8 | 166 | 31.7 | 5.6 | | | |
| | 9 | 193 | 9.9 | 3.9 | | | |
| | 10 | 205 | 16.0 | 7.5 | | | |
| | 11 | 224 | 31.8 | 5.4 | | | |
| | 12 | 241 | 27.3 | 5.6 | | | |
| | 13 | 258 | 102.0 | 8.3 | 256 | 1.9 | 21.1 |
| | 14 | 265 | 65.1 | 2.2 | 269 | 139. | 0.8 |
| | 15 | 272 | 160.0 | 4.9 | 277 | 75.1 | 4.5 |
| | 16 | 285 | 93.9 | 6.6 | 289 | 0.8 | 1.9 |
| | 17 | 303 | 20.6 | 9.2 | 308 | 0.7 | 0.2 |
| Sk –69D246 | 1 | 14 | 86.5 | 9.9 | 14 | 1.9 | 2.5 |
| | 2 | 19 | 14.6 | 1.9 | 20 | 3.5 | 1.6 |
| | 3 | | | | 25 | 34.1 | 1.3 |
| | 4 | 34 | 17.6 | 6.6 | | | |
| | 5 | 65 | 18.6 | 2.9 | 67 | 0.4 | 0.3 |
| | 6 | 73 | 9.2 | 5.3 | | | |
| | 7 | 116 | 6.1 | 4.4 | | | |
| | 8 | 139 | 5.1 | 4.3 | | | |
| | 9 | 182 | 30.4 | 17.4 | | | |
| | 10 | 195 | 6.3 | 2.3 | | | |
| | 11 | 218 | 24.6 | 6.8 | | | |
| | 12 | 231 | 66.3 | 5.2 | | | |
| | 13 | 240 | 22.3 | 2.9 | 239 | 0.9 | 10.4 |
| | 14 | 246 | 18.9 | 2.6 | 248 | 0.2 | 0.2 |
| | 15 | 254 | 40.4 | 4.5 | 256 | 0.2 | 2.0 |
| | 16 | 265 | 19.8 | 5.0 | | | |
| | 17 | 276 | 42.3 | 1.7 | 279 | 46.1 | 3.1 |
| | 18 | 280 | 217.0 | 7.8 | 285 | 17.4 | 5.5 |

Table 8. Logarithmic column densities of molecular hydrogen derived in the MW.

| | Sk –67D05 | Sk –68D135 | Sk –69D246 | AV 95 | Sk 159 |
|----------------------------------|-------------------------|-------------------------|-------------------------|-------------------------|-------------------------|
| $J=0$ | $14.40^{+0.15}_{-0.30}$ | $17.84^{+0.11}_{-0.05}$ | $18.40^{+0.04}_{-0.04}$ | $18.00^{+0.06}_{-0.06}$ | $15.70^{+0.30}_{-0.22}$ |
| $J=1$ | $15.11^{+0.22}_{-0.11}$ | $18.08^{+0.05}_{-0.04}$ | $18.46^{+0.04}_{-0.04}$ | $17.84^{+0.08}_{-0.08}$ | $16.17^{+0.30}_{-0.10}$ |
| $J=2$ | $14.30^{+0.24}_{-0.40}$ | $16.60^{+0.35}_{-0.10}$ | $16.30^{+0.10}_{-0.07}$ | $17.00^{+0.18}_{-0.15}$ | $14.78^{+0.43}_{-0.08}$ |
| $J=3$ | < 14.70 | $15.08^{+0.42}_{-0.08}$ | $15.70^{+0.08}_{-0.08}$ | $16.00^{+0.08}_{-0.08}$ | ... |
| $J=4$ | ... | $13.90^{+0.28}_{-0.43}$ | $14.23^{+0.07}_{-0.06}$ | $13.90^{+0.30}_{-0.43}$ | ... |
| Total | 15.30 ± 0.17 | 18.29 ± 0.05 | 18.73 ± 0.04 | 18.26 ± 0.05 | 16.31 ± 0.25 |
| T_{01} (K) | 136 | 103 | 83 | 66 | 153 |
| b_{Dopp} (km s ⁻¹) | 2.9; 2.4 ^a | 4.8 | 4.6 | 1.5 | 2.1 |

^a Two molecular components are detected towards Sk –67D05 at +35 km s⁻¹ and +39 km s⁻¹. We quote the total H₂ column densities.

Table 9. Logarithmic column densities of molecular and atomic species detected in the MCs^a.

| | Sk –67D05 | Sk –68D135 | Sk –69D246 | AV 95 | Sk 159 |
|--------------------------------------|-------------------------|-------------------------|-------------------------|-------------------------|-------------------------|
| H ₂ $J=0$ | $19.28^{+0.05}_{-0.06}$ | $19.46^{+0.10}_{-0.06}$ | $19.40^{+0.05}_{-0.04}$ | $19.11^{+0.04}_{-0.04}$ | $18.85^{+0.06}_{-0.08}$ |
| H ₂ $J=1$ | $18.93^{+0.04}_{-0.09}$ | $19.61^{+0.06}_{-0.04}$ | $19.30^{+0.04}_{-0.04}$ | $19.11^{+0.04}_{-0.04}$ | $18.95^{+0.06}_{-0.08}$ |
| H ₂ $J=2$ | $15.60^{+0.30}_{-0.30}$ | $18.48^{+0.12}_{-0.12}$ | $17.70^{+0.17}_{-0.50}$ | $17.81^{+0.05}_{-0.05}$ | $17.48^{+0.30}_{-0.10}$ |
| H ₂ $J=3$ | $15.25^{+0.25}_{-0.15}$ | $18.23^{+0.07}_{-0.08}$ | $17.70^{+0.20}_{-0.10}$ | $17.54^{+0.06}_{-0.07}$ | $17.03^{+1.30}_{-1.00}$ |
| H ₂ $J=4$ | $14.48^{+0.04}_{-0.06}$ | $17.48^{+0.12}_{-0.05}$ | $15.49^{+0.22}_{-0.17}$ | $16.54^{+0.12}_{-0.16}$ | $13.81^{+1.12}_{-0.40}$ |
| H ₂ $J=5$ | ... | $16.30^{+0.40}_{-0.07}$ | $15.17^{+0.45}_{-0.09}$ | $15.48^{+0.30}_{-0.13}$ | ... |
| H ₂ $J=6$ | ... | $14.54^{+0.20}_{-0.15}$ | $13.90^{+0.14}_{-0.12}$ | ... | ... |
| Total | 19.44 ± 0.05 | 19.87 ± 0.05 | 19.66 ± 0.04 | 19.43 ± 0.04 | 19.19 ± 0.06 |
| T_{01} (K) | 57 | 92 | 70 | 78 | 78 |
| b_{Dopp} (km s ⁻¹) | 5.1 | 4.4 | 3.6; 6.4 ^b | 0.8 | 1.0; 1.3 ^b |
| $N(\text{H}_{\text{total}})$ | 21.49 | 21.50 | 21.32 | 21.00 | ... |
| HD $J=0$ ^c | $13.62^{+0.09}_{-0.12}$ | $14.15^{+0.11}_{-0.15}$ | $13.62^{+0.07}_{-0.08}$ | $13.82^{+0.96}_{-0.18}$ | $13.85^{+0.11}_{-0.14}$ |
| CO ^c | $13.88^{+0.08}_{-0.09}$ | $13.77^{+0.20}_{-0.28}$ | $13.57^{+0.08}_{-0.09}$ | < 13.23 | < 13.34 |
| ClI | $13.87^{+0.12}_{-0.13}$ | $13.59^{+0.18}_{-0.20}$ | $13.46^{+0.24}_{-0.22}$ | $13.00^{+0.18}_{-0.30}$ | < 13.32 |
| ClII | < 13.78 | ... | $13.73^{+0.14}_{-0.05}$ | < 14.00 | ... |
| FeII | $14.84^{+0.20}_{-0.08}$ | $15.77^{+0.18}_{-0.30}$ | $15.26^{+0.11}_{-0.35}$ | $15.22^{+0.50}_{-0.50}$ | $14.93^{+0.50}_{-0.50}$ |
| χ ^d | 3 | 3,000 | 20 | 200 | 4 |
| distance (pc) | 120 | 5 | 28 | 3 | 50 |
| [Cl] | > 4.64 | 4.09 | 4.60 | 4.00 | ... |
| $\delta(\text{Cl})$ ^e | > -0.12 | -0.67 | -0.16 | > -0.70 | ... |
| ClI/H ₂ (total) (ppm) | 2.7 ± 0.9 | 0.5 ± 0.3 | 0.6 ± 0.4 | 0.4 ± 0.3 | < 1.3 |
| ClI/H ₂ ($J=0,1$) (ppm) | 2.7 ± 0.9 | 0.6 ± 0.3 | 0.6 ± 0.4 | 0.4 ± 0.3 | < 1.3 |
| HD/H ₂ (total) (ppm) | 1.5 ± 0.5 | 1.9 ± 0.8 | 0.9 ± 0.2 | [2.5...22.4] | 4.5 ± 1.8 |
| CO/H ₂ (total) (ppm) | 2.7 ± 0.7 | 0.8 ± 0.7 | 0.8 ± 0.2 | < 0.63 | < 1.33 |

^a All the errors quoted are 1 σ . The upper limits are 3 σ .

^b Two molecular components are detected towards Sk –69D246 and Sk 159.

^c Average between PF and AOD techniques.

^d The Interstellar Radiation Field (ISRF) at 1000 Å is given in Draine unit (7×10^{-17} erg cm⁻³ Å⁻¹).

^e The depletion of Chlorine, $\delta(\text{Cl})$, is the difference between the LMC and SMC values of 4.76 and 4.70, respectively (see Russell & Dopita 1992) and the values we derived here.

Table 10. S II and Fe II component parameters toward the SMC.

| Star | Comp | V_{hel} | N_{10} | b | V_{hel} | N_{11} | b |
|--------|------|------------------|-------------------------|--------------------|------------------|-------------------------|--------------------|
| | | Fe II | 10^{14}cm^{-2} | km s^{-1} | S II | 10^{14}cm^{-2} | km s^{-1} |
| AV 95 | 1 | -15 | $> 12.0^a$ | $< 15.0^a$ | | | |
| | 2 | 10 | 4.7 | 8.9 | 7 | 11.1 | 9.1 |
| | 3 | | | | 15 | 11.3 | 5.9 |
| | 4 | 48 | 2.4 | 4.7 | 52 | 31.0 | 0.3 |
| | 5 | 75 | $> 0.9^a$ | $< 11.^a$ | 75 | 1.0 | 4.4 |
| | 6 | | | | 85 | 1.6 | 5.1 |
| | 7 | 95 | 9.7 | 17.4 | 99 | 8.7 | 8.1 |
| | 8 | 123 | 7.1 | 16.8 | 119 | $> 20.0^a$ | $< 11.0^a$ |
| | 9 | | | | 134 | 9.0 | 7.7 |
| | 10 | 169 | 0.9 | 28.6 | | | |
| | 11 | 195 | $> 0.6^a$ | $< 21.0^a$ | | | |
| Sk 159 | 1 | -2. | 1.1 | 2.5 | | | |
| | 2 | 23 | 8.1 | 16.9 | | | |
| | 3 | 150 | 8.6 | ... ^b | | | |

^a Lower and upper limits quoted are 3σ .^b For this very saturated component the possible b -value ranges from 1 to 40 km s^{-1} .

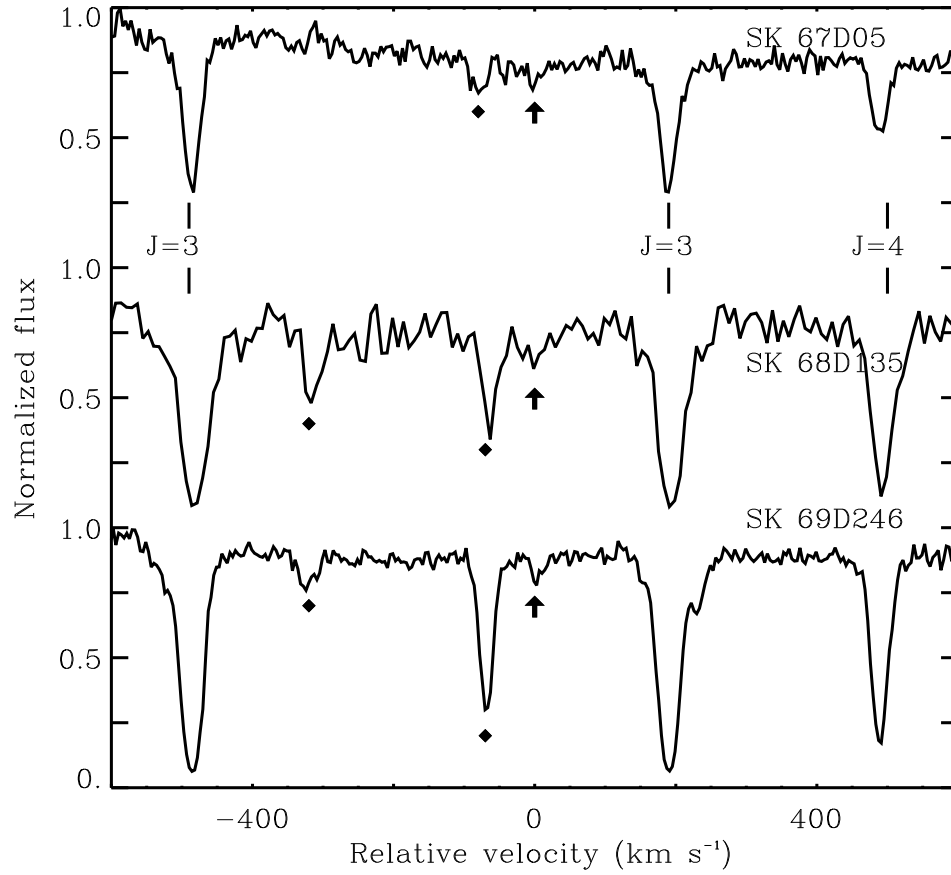


Fig. 1. Detection of the 1043 Å HD ($J = 0$) line in the LMC. H₂ Rotational levels 3 and 4 are indicated for the LMC component while the black diamonds point to the strongest H₂ features from the Galactic component. The velocities are shifted so that the $\lambda 1043$ Å HD line appears at 0 km s⁻¹.

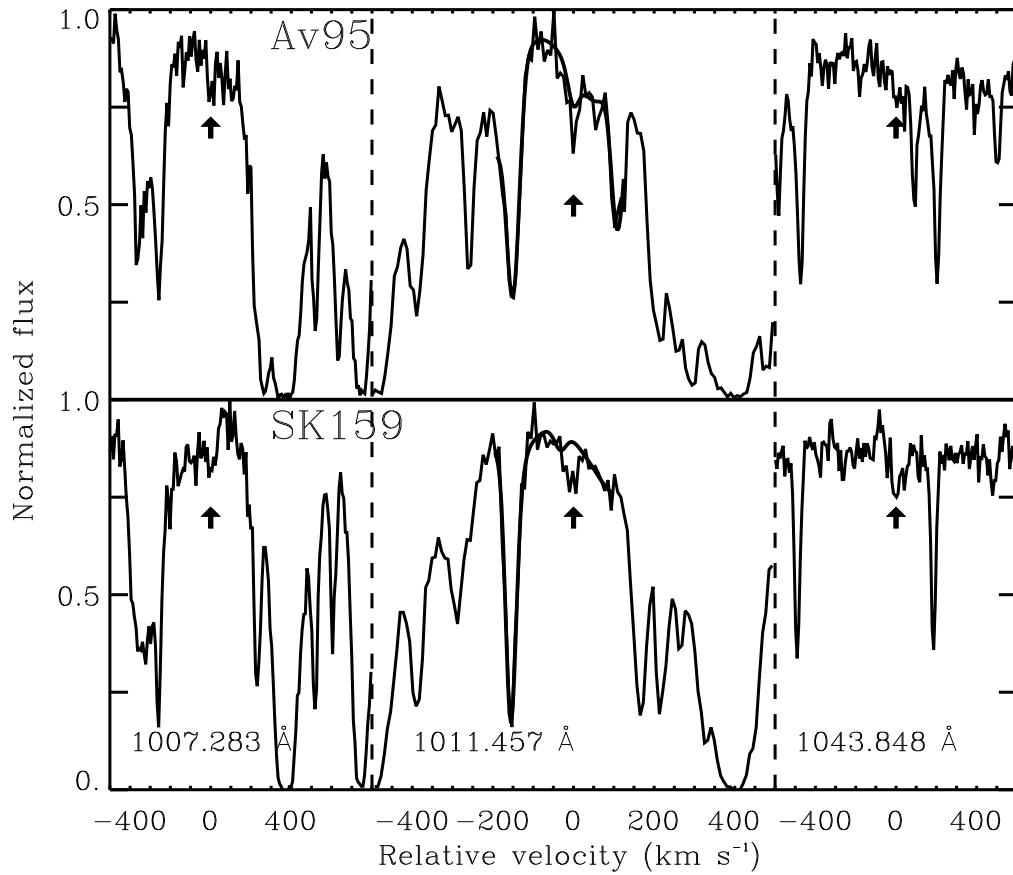


Fig. 2. Detections of the HD molecule towards the SMC at three different wavelengths. AOD analysis is based on the 1007 Å HD transition. For clarity we overplotted the profile fitting model over the 1011 Å transition which is blended by a Galactic H₂ line. The velocities are shifted so that the HD lines appear at 0 km s⁻¹ in each case.

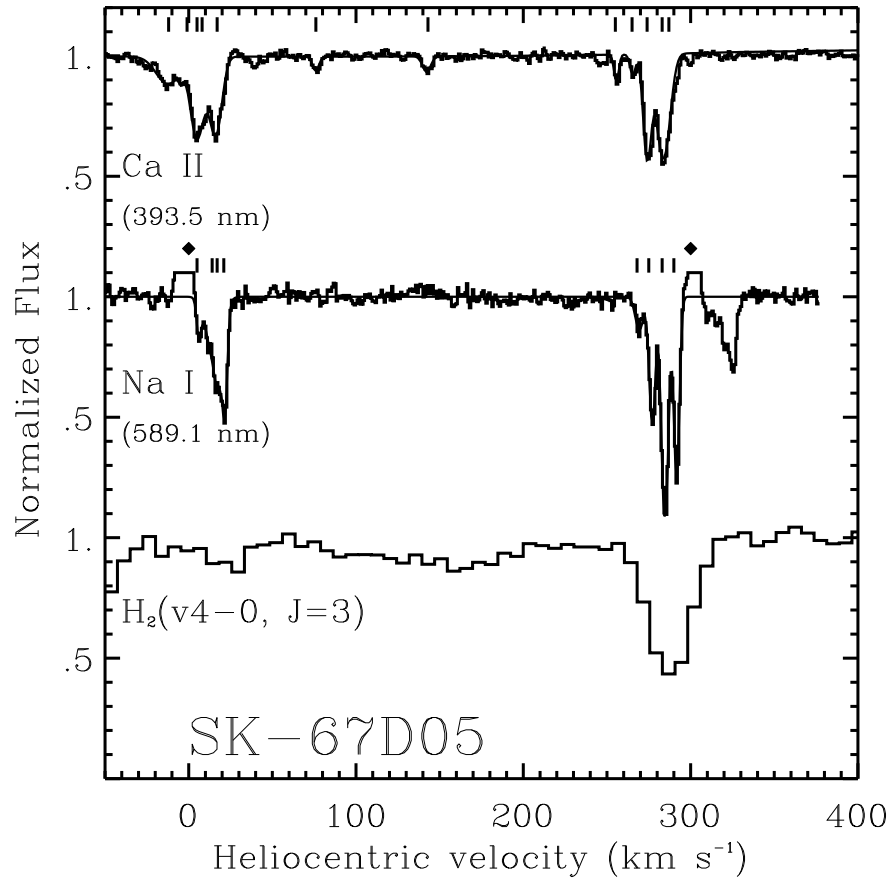


Fig. 3. VLT/UVES data for Na and Ca shows up to 14 components, 5 of them arising in the MW. Two distinct groups of absorbers show up in the spectra: Galactic at $\approx +10 \text{ km s}^{-1}$ and LMC at $\approx +290 \text{ km s}^{-1}$. Only two weak intermediate velocity absorbers are detected in Ca II. Na I airglows have been truncated and indicated with diamonds. Note that the fits of Na I have been performed on both lines of the doublet. Part of the second doublet is seen in the far left of the spectrum displayed.

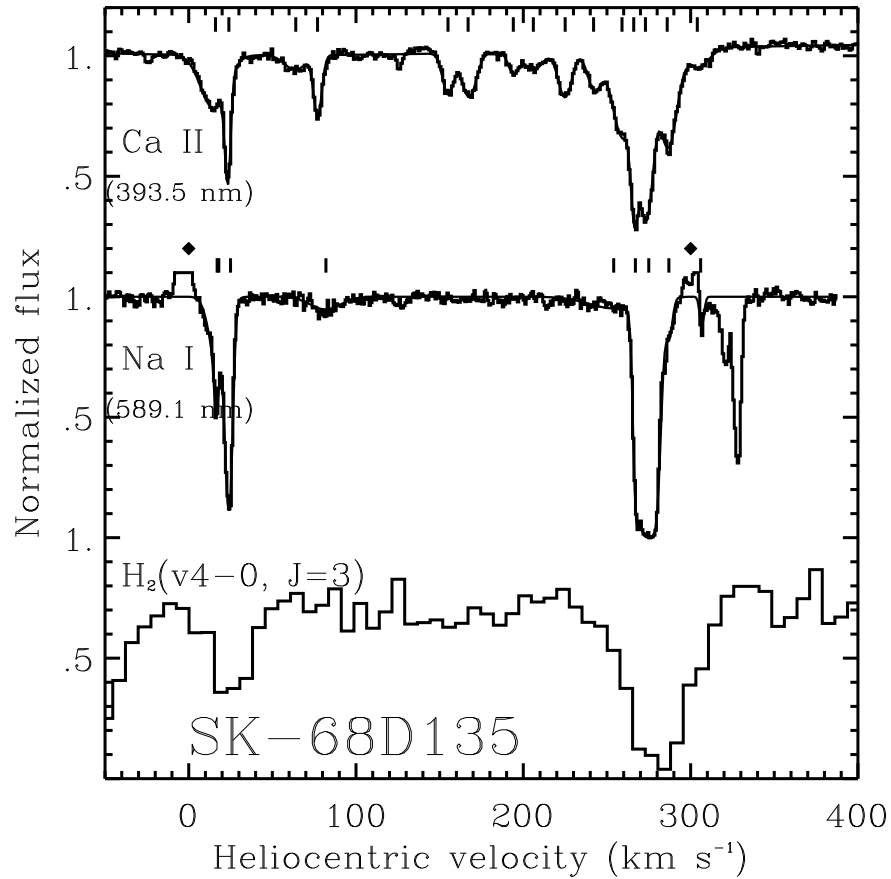


Fig. 4. The sightline towards Sk-68D135 is similar to the sightline towards Sk-69D246 with two groups of strong NaI absorbers: Galaxy and LMC. The FUSE molecular data are consistent with a single molecular absorber in the LMC but the resolution is not sufficient to discard the existence of a more complex structure. Note the HVC NaI and CaII components around +310 km s⁻¹. Na I airglows have been truncated and indicated with diamonds.

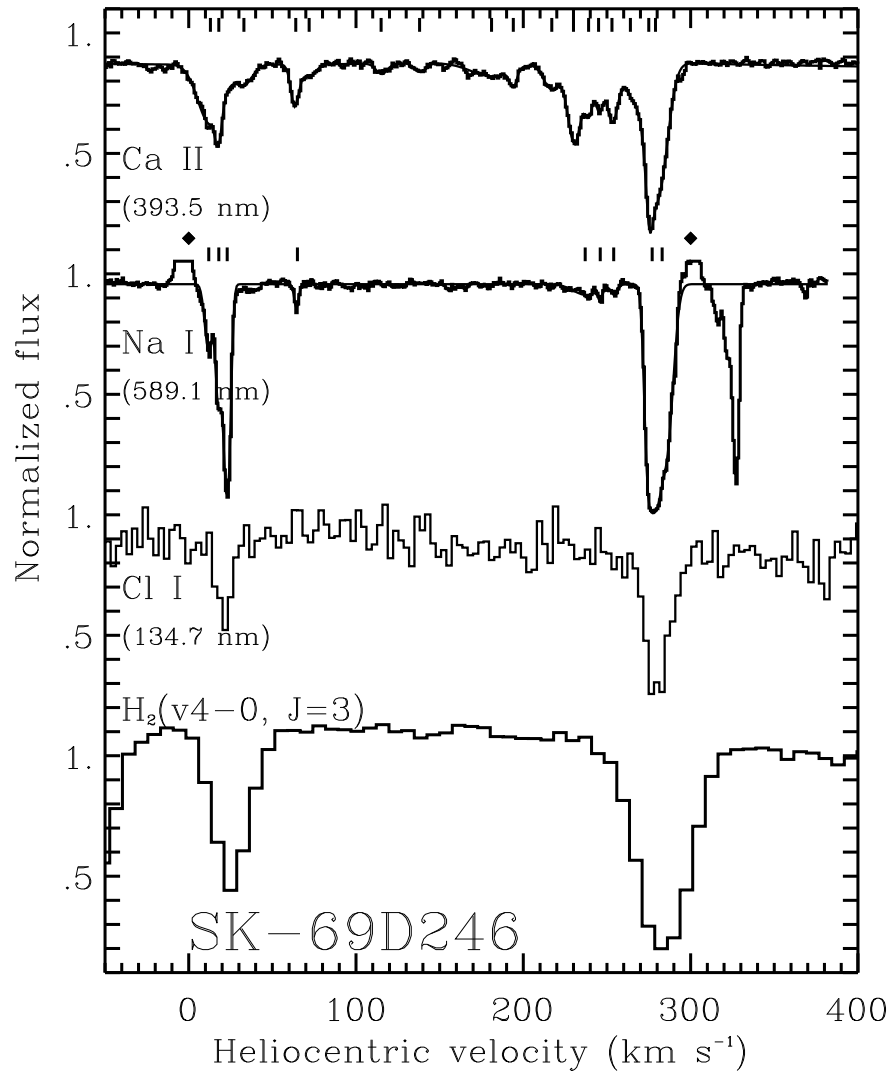


Fig. 5. With 19 components this sightline has the most complicated velocity structure of the sample. Note that with VLT/UVES, STIS and FUSE data, this sightline is also the one for which we have the most complete information about the velocity structure. Note also that the last 2 CaII, NaI and H₂ components coincide more or less in the profile fitting. Na I airglows have been truncated and indicated with diamonds.

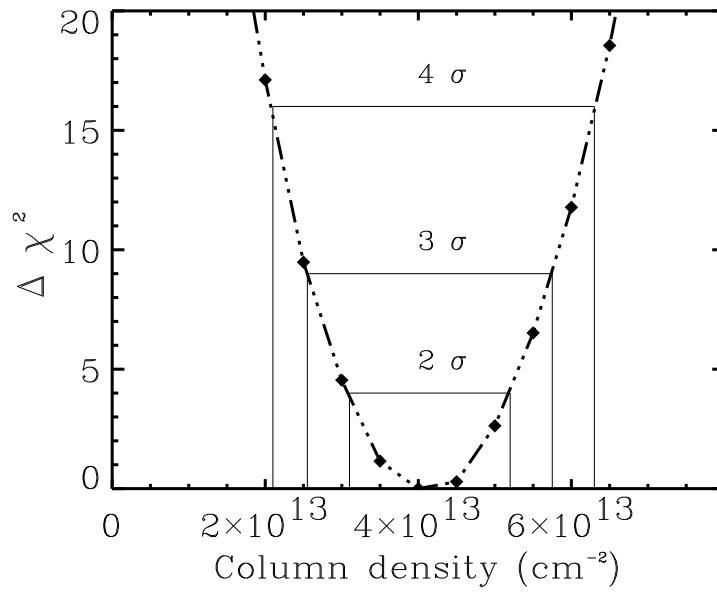


Fig. 6. χ^2 plot from the profile fitting of HD towards Sk-69D246. 2σ error bars are calculated with the standard $\Delta\chi^2$ method. Note that for this fit the $\overline{\chi^2}$ is very close to unity.

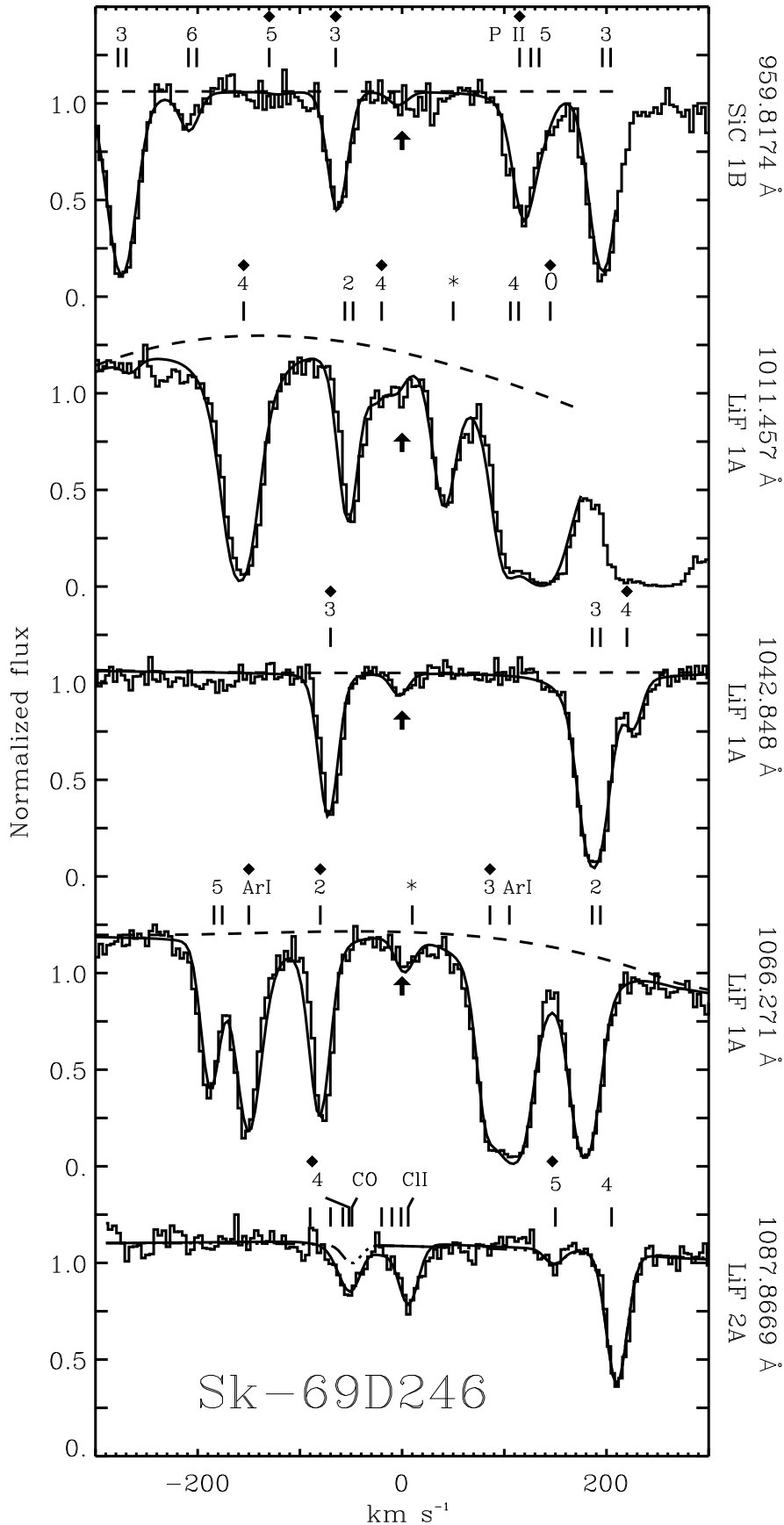


Fig. 7. Examples of profiles fitted on the FUSE data for Sk-69D246. Galactic absorption lines are indicated by the black diamonds and the unidentified stellar features by the stars. The spectra are centered on the LMC HD lines except for the last plot which is centered on the LMC CII line. Note the $J = 4$ Galactic absorption over the profile of the LMC CO absorption. Note also the numerous CO rotational levels (not labeled) spreading over 100 km s^{-1} .

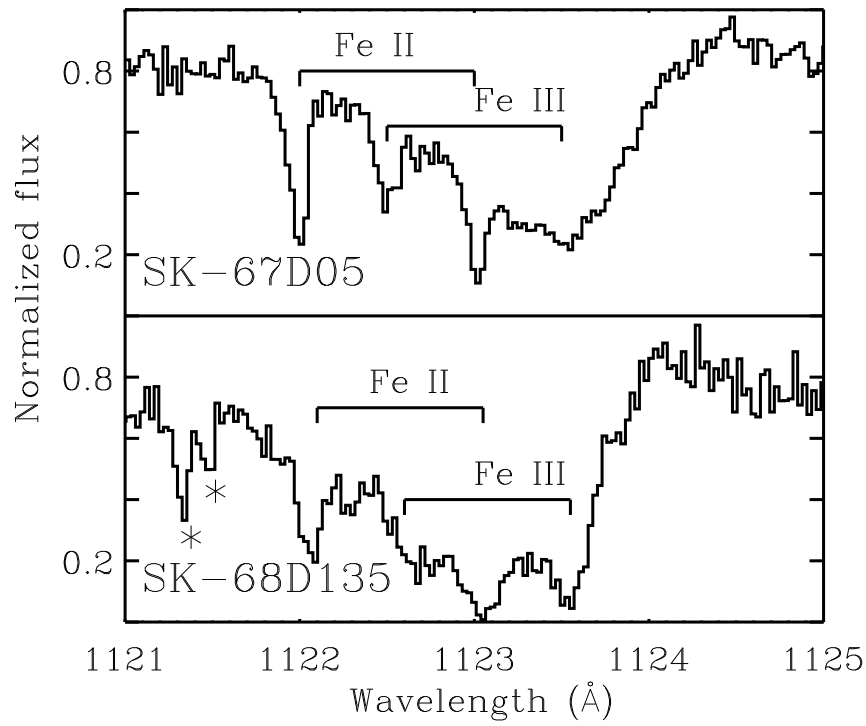


Fig. 8. The Fe II and Fe III absorption features arising in the MW and in the LMC towards Sk-68D135 (bottom panel) and Sk-67D05 (upper panel). Although the LMC Fe III line is barely seen towards Sk-67D05, we can see a strong detection towards Sk-68D135 consistent with the intense radiation field.

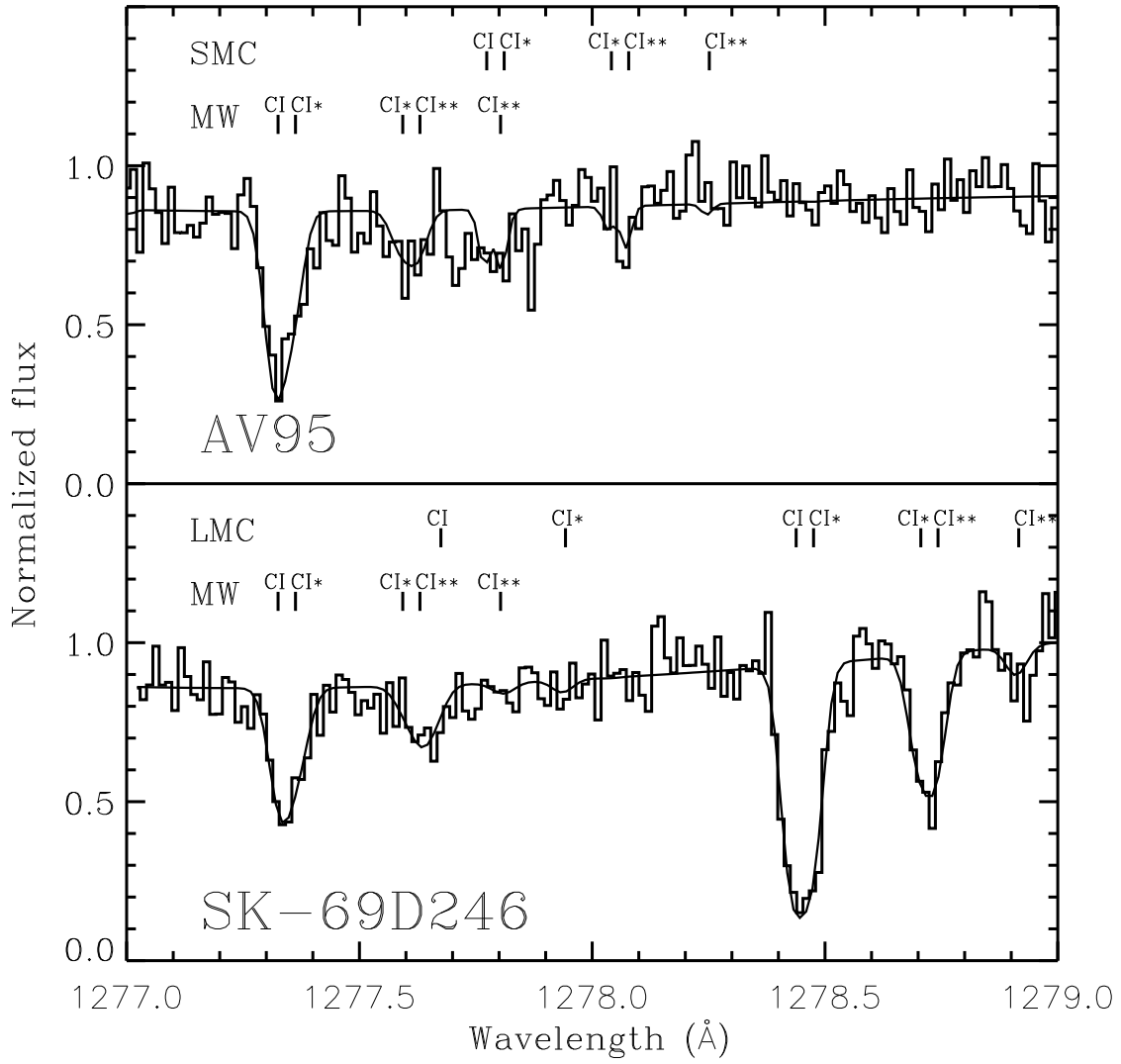


Fig. 9. Profile fitting of the carbon lines detected in the STIS data towards AV 95 and Sk -69D246.

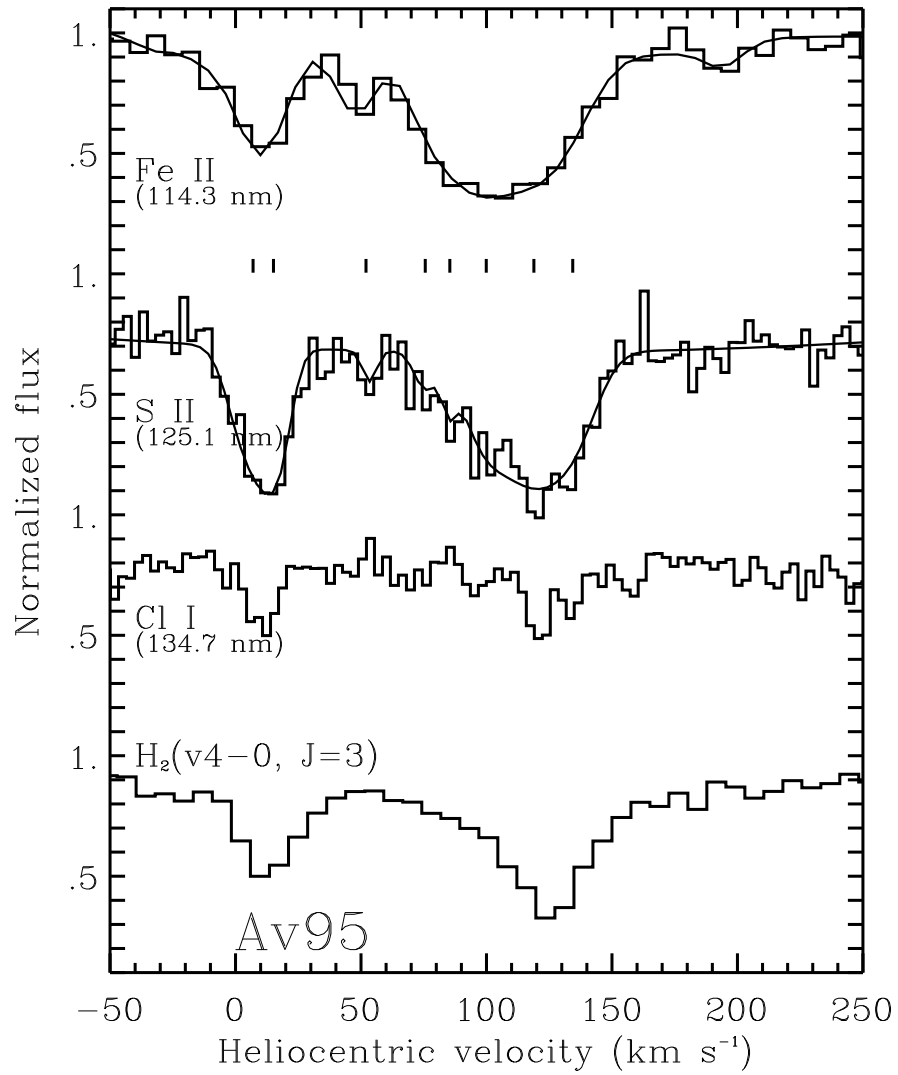


Fig. 10. Atomic and molecular velocity structures towards AV95 as derived from STIS S II and FUSE Fe II and H₂ data. Up to 11 atomic components are identified combining sulfur and iron absorbers. Note that with a resolution of 20 km s⁻¹ many Fe II absorbers might well not be resolved and the Fe II column densities are uncertain. As to the molecular component, observations of Cl I with STIS at ≈ 6 km s⁻¹ are consistent with a single molecular cloud.

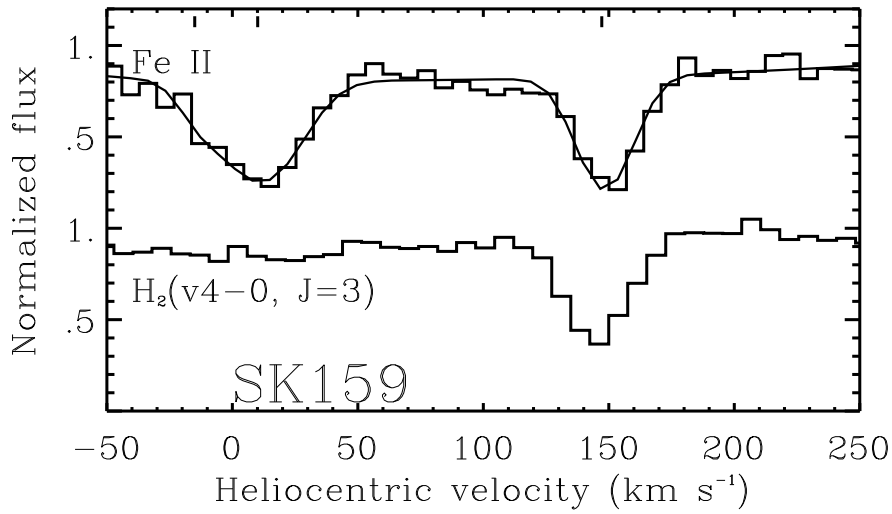


Fig. 11. Atomic and molecular velocity structures towards Sk159. Based on the FUSE data itself, only one SMC absorber is revealed. However, higher resolution data, obtained at the 3.6 CES at ESO Chile, shows that there are at least 2 atomic absorbers present along the sightline at +144 and +149 km s⁻¹ (Sylvi 1996).

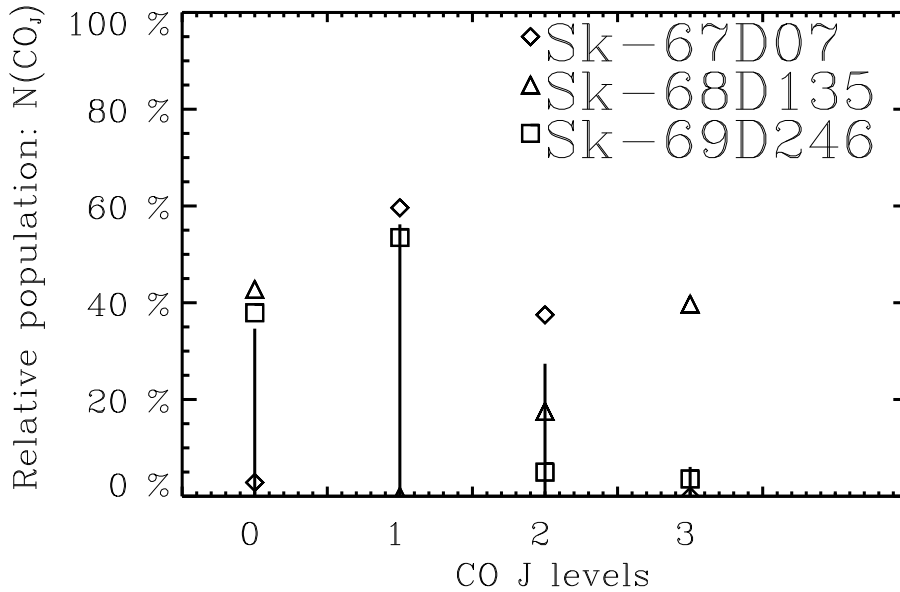


Fig. 12. The relative population distribution of the CO $J = 1-3$ lines derived from the observations is compared to a theoretical Boltzmann distribution at $T_{ex}(\text{CO}) = 9$ K. The agreement is relatively good although the error bars on the individual measurements are of the order of 50 % (not shown).